

## **ASSOCIATE EDITOR**

*I am pleased to announce that both of the two reviewers have recommended publication with minor revisions. Please carefully address the last few technical and methodological comments by the reviewers and provide me with a complete list of your responses to the reviewer comments that either clearly refer to changes in the final revision or explain, where you refrained from changing the manuscript according to the reviewer suggestions.*

*Append a track changes version and a final version of your revised manuscript.*

**Response:** We answered all points raised by the reviewers and made the requested changes.

## **REFEREE 1**

*I thank the authors for taking into account my concerns.*

*Regarding the differences between topsoil and tree alleys, the results are now clearer. Thanks for the new Fig. 2 in the replies. This shows nicely that the differences are almost entirely in topsoil and only for the tree row (but also reinforces my concerns for numerical errors in topsoil because of the strong gradients compared to the used resolution). I think this figure is necessary and should be added to the manuscript, because it helps to clarify the results and sets the context for comparing agroforestry with control. The wording in the abstract needs to reflect this too (L 34ff).*

**Response:** This figure was added to the manuscript (P8, Fig. 1). The following sentence was added to the abstract: “However, most of the SOC storage occurred in the first 30 cm of soil and the tree rows.” (P2-L34-35).

*Regarding depth resolution, Fig. 1 in reply dampens my concerns on numeric error, as it suggests some robustness. Please, add some discussion to the manuscript on this point in addition to the reply.*

**Response:** The following sentence was added into the discussion: “The strong SOC gradient observed in the topsoil in tree rows compared to the used resolution could lead to numerical errors. We therefore tested a finer grid resolution, and results were very similar, suggesting some robustness of the model.” (P39-L749-752).

*Regarding the priming effects, it is kind to omit the interpretation from the manuscript that I was not able to follow.*

**Response:** Thank you. If the reviewer was not able to understand this part, future readers would also have had the same troubles. The best decision was to remove it from the manuscript as it was not the core message.

*Regarding the prior information, I am still confused and have still concerns, see below.*

*You seem not be interested in prior and posterior parameter distributions. To my reading, rather, a prior-like term is used to regularize the cost function. Hence, I suggest to avoid the term Bayesian. The result stay valid also with a gradient based optimization.*

**Response:** When referring to the optimization procedure, the term Bayesian was removed and replaced by “gradient based optimization” (P25-L551-552, P26-L565).

*In the reply on my questions regarding the prior you write about starting parameters for the gradient search instead of prior knowledge on parameters. That is why I am still confused. Starting parameters are a very different thing from priors on parameters. Its good practice to vary the starting values of a gradient search, but its conceptually wrong to randomly vary prior parameter values (aside from testing whether your prior has a significant impact on the posterior.)*

**Response:** To avoid confusion we modified the term “prior” to “starting parameter” in the entire manuscript (P26-L569-571, P26-L575-576, P26-L582, P32 Table 5, P34-L662).

*Did you vary also the prior parameter values in  $x_b$  and the P-Matrix (eq. 34) during optimization? To my opinion an optimized prior would be conceptually not acceptable and I would request to redo the optimization with fixed values of  $x_b$  and P. This is true for both, a Bayesian analysis and for a regularization of the cost function. Still you need to document values of P (at least diagonals). Or you may omit the prior term in eq. 34 altogether, if you do not need a regularization. If you are not able to redo the optimization, please, clearly describe what you have done with the priors ( $x_b$  and P in eq. 34), maybe in an appendix. Although, varying priors is conceptually wrong, you may be confident that it does not have a big effect on results and does not impair conclusions.*

**Response:** No, the starting parameter values were fixed in eq. 34, we clarified this point in the manuscript: ‘ $x_b$  the vector of a starting parameter values fixed for each optimization procedures,’ (P26-L575-576). The P-matrix were added in the supplementary materials.

*Please, be precise when speaking about prior parameter values in the cost function ( $x_b$ ) versus starting values for the optimization.*

**Response:** To avoid confusion we modified the term “prior” to “starting parameter” in the entire manuscript (P26-L569-571, P26-L575-576, P26-L582, P32 Table 5, P34-L662).

*Tab 5: If the optimization is done at original (not log) scale, I suggest to also present the results at original scale.*

**Response:** Table 5 was modified to the previous version of the manuscript (P32).

*L34: The wording suggests that the stocks in the agroforestry plot are increased across all the area and all the depth. While this is true for a total comparison, I strongly suggest rewording so that the facts from new Fig 2 (mainly topsoil, mainly tree alleys) become clearer.*

**Response:** The following sentence was added to the abstract: “However, most of the SOC storage occurred in the first 30 cm of soil and the tree rows.” (P2-L34-35).

## **REFEREE 2**

*I have reviewed this manuscript once more following the additional revisions. I think the authors have adequately addressed the additional comments, although I am not qualified to judge the issue raised by the other reviewer regarding the use of different priori values in the Bayesian analysis and the use of the BFGS over the suggested MCMC, this evaluation must therefore rely on the other reviewer's assessment. While this study includes some limitations and simplifying assumptions, I think the authors have made sufficient effort in outlining and considering these in the revised manuscript version. Overall this study is a valuable contribution to the scientific literature in my opinion. I have just one minor comment regarding the revised abstract where the deletion of one sentence has created some confusing statement suggesting that 'the priming effect variant being able to capture the SOC depth distribution ...questions the potential of soil to store C' (lines 37-39). Since these two sentences did not refer to each other in the original abstract, the authors should carefully reconsider the wording and link between these remaining sentences in the revised abstract.*

**Response:** Thank you for you kind comments. We rephrased this sentence as requested: “Moreover, only a priming effect variant of the model was able to capture the depth distribution of SOC stocks, suggesting priming effect as a possible mechanism driving deep SOC dynamics. This result questions the potential of soils to store large amounts of carbon, especially at depth.” (P2-L38-40).

1 **High organic inputs explain shallow and deep SOC storage in a long-term agroforestry**  
2 **system – Combining experimental and modeling approaches.**

3

4 Rémi Cardinael<sup>a,b,c,d\*</sup>, Bertrand Guenet<sup>e</sup>, Tiphaine Chevallier<sup>a</sup>, Christian Dupraz<sup>f</sup>, Thomas  
5 Cozzi<sup>b</sup>, Claire Chenu<sup>b</sup>

6

7 <sup>a</sup> Eco&Sols, IRD, CIRAD, INRA, Montpellier SupAgro, Univ Montpellier, Montpellier, France

8 <sup>b</sup> AgroParisTech, UMR Ecosys, Avenue Lucien Brétignières, 78850 Thiverval-Grignon, France

9 <sup>c</sup> CIRAD, UPR AIDA, F-34398 Montpellier, France (present address)

10 <sup>d</sup> AIDA, Univ Montpellier, CIRAD, Montpellier, France

11 <sup>e</sup> Laboratoire des Sciences du Climat et de l'Environnement, UMR CEA-CNRS-UVSQ, CE

12 L'Orme des Merisiers, 91191 Gif-Sur-Yvette, France

13 <sup>f</sup> System, INRA, CIRAD, Montpellier SupAgro, Univ Montpellier, Montpellier, France

14 \* Corresponding author. Tel.: +33 04.67.61.53.08. E-mail address: remi.cardinael@cirad.fr

15

16 *Keywords:* priming effect, deep roots, deep soil organic carbon, spatial heterogeneity,  
17 silvoarable system, crop yield, SOC modeling

18

19 **Abstract**

20 Agroforestry is an increasingly popular farming system enabling agricultural diversification

21 and providing several ecosystem services. In agroforestry systems, soil organic carbon (SOC)

22 stocks are generally increased, but it is difficult to disentangle the different factors responsible

23 for this storage. Organic carbon (OC) inputs to the soil may be larger, but SOC decomposition

24 rates may be modified owing to microclimate, physical protection, or priming effect from roots,

25 especially at depth. We used an 18-year-old silvoarable system associating hybrid walnut trees

26 (*Juglans regia* × *nigra*) and durum wheat (*Triticum turgidum* L. subsp. *durum*), and an adjacent  
27 agricultural control plot to quantify all OC inputs to the soil - leaf litter, tree fine root  
28 senescence, crop residues, and tree row herbaceous vegetation -, and measure SOC stocks down  
29 2 m depth at varying distances from the trees. We then proposed a model that simulates SOC  
30 dynamics in agroforestry accounting for both the whole soil profile and the lateral spatial  
31 heterogeneity. The model was calibrated to the control plot only.  
32 Measured OC inputs to soil were increased by about 40% (+ 1.11 t C ha<sup>-1</sup> yr<sup>-1</sup>) down to 2 m  
33 depth in the agroforestry plot compared to the control, resulting in an additional SOC stock of  
34 6.3 t C ha<sup>-1</sup> down to 1 m depth. However, most of the SOC storage occurred in the first 30 cm  
35 of soil and in the tree rows. The model was strongly validated, describing properly the measured  
36 SOC stocks and distribution with depth in agroforestry tree rows and alleys. It showed that the  
37 increased inputs of fresh biomass to soil explained the observed additional SOC storage in the  
38 agroforestry plot. Moreover, only a priming effect variant of the model was able to capture the  
39 depth distribution of SOC stocks, suggesting priming effect as a possible mechanism driving  
40 deep SOC dynamics. This result questions the potential of soils to store large amounts of  
41 carbon, especially at depth. Deep-rooted trees modify OC inputs to soil, a process that deserves  
42 further studies given its potential effects on SOC dynamics.

43

## 44 **1 Introduction**

45 Agroforestry systems are complex agroecosystems combining trees and crops or pastures  
46 within the same field (Nair, 1993, 1985; Somarriba, 1992). More precisely, silvoarable systems  
47 associate parallel tree rows with annual crops. Some studies showed that these systems could  
48 be very productive, with a land equivalent ratio (Mead and Willey, 1980) reaching up to 1.3  
49 (Graves et al., 2007). Silvoarable systems may therefore produce up to 30% more marketable  
50 biomass on the same area of land compared to crops and trees grown separately. This

51 performance can be explained by a better use of water, nutrients and light by the agroecosystem  
52 throughout the year. Trees grown in silvoarable systems usually grow faster than the same trees  
53 grown in forest ecosystems, because of their lower density, and because they also benefit from  
54 the crop fertilization (Balandier and Dupraz, 1999; Chaudhry et al., 2003; Chiffot et al., 2006).  
55 In temperate regions, farmers usually grow one crop per year, and this association of trees can  
56 extend the growing period at the field scale, especially when winter crops are intercropped with  
57 trees having a late bud break (Burgess et al., 2004). However, after several years, a decrease of  
58 crop yield can be observed in mature and highly dense plantations, especially close to the trees,  
59 due to competition between crops and trees for light, water, and nutrients (Burgess et al., 2004;  
60 Dufour et al., 2013; Yin and He, 1997).

61 Part of the additional biomass produced in agroforestry is used for economical purposes, such  
62 as timber or fruit production. Leaves, tree fine roots, pruning residues and the herbaceous  
63 vegetation growing in the tree rows will usually return to the soil, contributing to a higher input  
64 of organic carbon (OC) to the soil compared to an agricultural field (Peichl et al., 2006).

65 In such systems, the observed soil organic carbon (SOC) stocks are also generally higher  
66 compared to a cropland (Albrecht and Kandji, 2003; Kim et al., 2016; Lorenz and Lal, 2014).  
67 Cardinael *et al.*, (2017) measured a mean SOC stock accumulation rate of 0.24 (0.09-0.46) t C  
68 ha<sup>-1</sup> yr<sup>-1</sup> at 0-30 cm depth in several silvoarable systems compared to agricultural plots in  
69 France. Higher SOC stocks were also found in Canadian agroforestry systems, but measured  
70 only to 20 cm depth (Bambrick et al., 2010; Oelbermann et al., 2004; Peichl et al., 2006).

71 To our knowledge, we are still not able to disentangle the factors responsible for such a higher  
72 SOC storage. This SOC storage might be due to higher OC inputs but it could also be favored  
73 by a modification of the SOC decomposition owing to a change in SOC physical protection  
74 (Haile et al., 2010), and/or in soil temperature and moisture.

75 The introduction of trees in an agricultural field modifies the amount, but also the distribution  
76 of fresh organic carbon (FOC) input to the soil, both vertically and horizontally (Bambrick et  
77 al., 2010; Howlett et al., 2011; Peichl et al., 2006). FOC inputs from the trees decrease with  
78 increasing distance from the trunk and with soil depth (Moreno et al., 2005). On the contrary,  
79 crop yield usually increases with increasing distance from the trees (Dufour et al., 2013; Li et  
80 al., 2008). Therefore, the proportions of FOC coming from both the crop residues and the trees  
81 change with distance from the trees, soil depth, and time.

82 Tree fine roots (diameter  $\leq 2$  mm) are the most active part of root systems (Eissenstat and Yanai,  
83 1997) and play a major role in carbon cycling. In silvoarable systems, tree fine root distribution  
84 within the soil profile is strongly modified due to the competition with the crop, inducing a  
85 deeper rooting compared to trees grown in forest ecosystems (Cardinael et al., 2015a; Mulia  
86 and Dupraz, 2006). Deep soil layers may therefore receive significant OC inputs from fine root  
87 mortality and exudates. Root carbon has a higher mean residence time in the soil compared to  
88 shoot carbon (Kätterer et al., 2011; Rasse et al., 2006), presumably because root residues are  
89 preferentially stabilized within microaggregates or adsorbed to clay particles. Moreover,  
90 temperature and moisture conditions are more buffered in the subsoil than in the topsoil. The  
91 microbial biomass is also smaller at depth (Eilers et al., 2012; Fierer et al., 2003), and the spatial  
92 segregation with organic matter is larger (Salomé et al., 2010) resulting in lower decomposition  
93 rates. Deep root carbon input in the soil could therefore contribute to a SOC storage with high  
94 mean residence times. However, some studies showed that adding FOC – a source of energy  
95 for microorganisms - to the subsoil enhanced decomposition of stabilized carbon, a process  
96 called « priming effect » (Fontaine et al., 2007). The priming effect is stronger when induced  
97 by labile molecules like root exudates than by root litter coming from the decomposition of  
98 dead roots (Shahzad et al., 2015). Therefore, the net effect of deep roots on SOC stocks has to  
99 be assessed, especially in silvoarable systems.

100 Models are crucial as they allow virtual experiments to best design and understand complex  
101 processes in these systems (Luedeling et al., 2016). Several models have been developed to  
102 simulate interactions for light, water and nutrients between trees and crops (Charbonnier et al.,  
103 2013; Duursma and Medlyn, 2012; van Noordwijk and Lusiana, 1999; Talbot, 2011) or to  
104 predict tree growth and crop yield in agroforestry systems (Graves et al., 2010; van der Werf et  
105 al., 2007). However, none of these models are designed to simulate SOC dynamics in  
106 agroforestry systems and they are therefore not useful to estimate SOC storage. Oelbermann &  
107 Voroney (2011) evaluated the ability of the CENTURY model (Parton et al., 1987) to predict  
108 SOC stocks in tropical and temperate agroforestry systems, but with a single-layer modeling  
109 approach (0-20 cm). The approach of modeling a single topsoil layer assumes that deep SOC  
110 does not play an active role in carbon cycling, while it was shown that deep soil layers contain  
111 important amounts of SOC (Jobbagy and Jackson, 2000), and that part of this deep SOC could  
112 cycle on decadal timescales due to root inputs or to dissolved organic carbon transport (Baisden  
113 and Parfitt, 2007; Koarashi et al., 2012). The need to take into account deep soil layers when  
114 modeling SOC dynamics is now well recognized in the scientific community (Baisden et al.,  
115 2002; Elzein and Balesdent, 1995), and several models have been proposed (Braakhekke et al.,  
116 2011; Guenet et al., 2013; Koven et al., 2013; Taghizadeh-Toosi et al., 2014; Ahrens et al.,  
117 2015). Using vertically discretized soils is particularly important when modeling the impact of  
118 agroforestry systems on SOC stocks, but to our knowledge, vertically spatialized SOC models  
119 have not yet been tested for these systems.

120

121 The aims of this study were then twofold: (i) to propose a model of soil C dynamics in  
122 agroforestry systems able to account for both vertical and lateral spatial heterogeneities and (ii)  
123 to test whether variations of fresh organic carbon (FOC) input could explain increased SOC  
124 stocks both using experimental data and model runs.



125 For this, we first compiled data on FOC inputs to the soil obtained in a 18-year-old agroforestry  
126 plot and in an agricultural control plot in southern France, in which SOC stocks have been  
127 recently quantified to 2 m depth (Cardinael et al., 2015b). FOC inputs comprised tree fine roots,  
128 tree leaf litter, aboveground and belowground biomass of the crop and of the herbaceous  
129 vegetation in the tree rows. We compiled recently published data for FOC inputs (Cardinael et  
130 al., 2015a; Germon et al., 2016), and measured the others (Table 1).

131

132 We then modified a two pools model proposed by Guenet *et al.*, (2013), to create a spatialized  
133 model over depth and distance from the tree, the CARBOSAF model (soil organic CARBOn  
134 dynamics in Silvoarable AgroForestry systems). Based on data acquired since the tree planting  
135 in 1995 (crop yield, tree growth), and on FOC inputs, we modeled SOC dynamics to 2 m depth  
136 in both the silvoarable and agricultural control plot. We evaluated the model against measured  
137 SOC stocks along the profile and used this opportunity to test the importance of priming effect  
138 (*PE*) for deep soil C dynamics in a silvoarable system. The performance of the two pools model  
139 including *PE* was also compared with a model version including three OC pools.

140

## 141 **2 Materials and methods**

### 142 **2.1 Study site**

143 The experimental site is located at the Restinclières farm Estate in Prades-le-Lez, 15 km North  
144 of Montpellier, France (longitude 04°01' E, latitude 43°43' N, elevation 54 m a.s.l.). The  
145 climate is sub-humid Mediterranean with an average temperature of 15.4°C and an average  
146 annual rainfall of 973 mm (years 1995–2013). The soil is a silty and carbonated (pH = 8.2) deep  
147 alluvial Fluvisol (IUSS Working Group WRB, 2007). In February 1995, a 4.6 hectare  
148 silvoarable agroforestry plot was established with the planting of hybrid walnut trees (*Juglans*  
149 *regia* × *nigra* cv. NG23) at a density of 192 trees ha<sup>-1</sup> but later thinned to 110 trees ha<sup>-1</sup>. Trees

150 were planted at 13 m × 4 m spacing, and tree rows are East–West oriented. The cultivated alleys  
 151 are 11 m wide. The remaining part of the plot (1.4 ha) was kept as an agricultural control plot.  
 152 Since the tree planting, the agroforestry alleys and the control plot were managed in the same  
 153 way. The associated crop is most of the time durum wheat (*Triticum turgidum* L. subsp. *durum*),  
 154 except in 1998, 2001 and 2006, when rapeseed (*Brassica napus* L.) was cultivated, and in 2010  
 155 and 2013, when pea (*Pisum sativum* L.) was cultivated. The soil is ploughed to a depth of 0.2  
 156 m before sowing, and the wheat crop is fertilized with an average of 120 kg N ha<sup>-1</sup> yr<sup>-1</sup>. Crop  
 157 residues (wheat straw) are also exported, but about 25% remain on the soil. Tree rows are  
 158 covered by spontaneous herbaceous vegetation. Two successive herbaceous vegetation types  
 159 occur during the year, one in summer and one in winter. The summer vegetation is mainly  
 160 composed of *Avena fatua* L., and is 1.5 m tall. In winter, the vegetation is a mix of *Achillea*  
 161 *millefolium* L., *Galium aparine* L., *Vicia* L., *Ornithogalum umbellatum* L. and *Avena fatua* L.,  
 162 and is 0.2 m tall.

163

164 **Table 1.** Synthesis of the different field and laboratory data available or measured, and their  
 165 sources.

Description of the data	Source
Soil texture, bulk densities, SOC stocks	Cardinael <i>et al.</i> , (2015a)
Soil temperature and soil moisture	Measured
Tree growth (DBH)	Measured
Tree wood density	(Talbot, 2011)
Tree fine root biomass	Cardinael <i>et al.</i> , (2015b)
Tree fine root turnover	Germon <i>et al.</i> , (2016)
Crop yield and crop ABG biomass	Dufour <i>et al.</i> , (2013) and measured
Crop root biomass	Prieto <i>et al.</i> , (2015) and measured
Tree row herbaceous vegetation – ABG biomass	Measured
Tree row herbaceous vegetation – root biomass	Measured
Biomass carbon concentrations	Measured
Potential decomposition rate of roots	Prieto <i>et al.</i> , (2016a)
HSOC potential decomposition rate	Measured

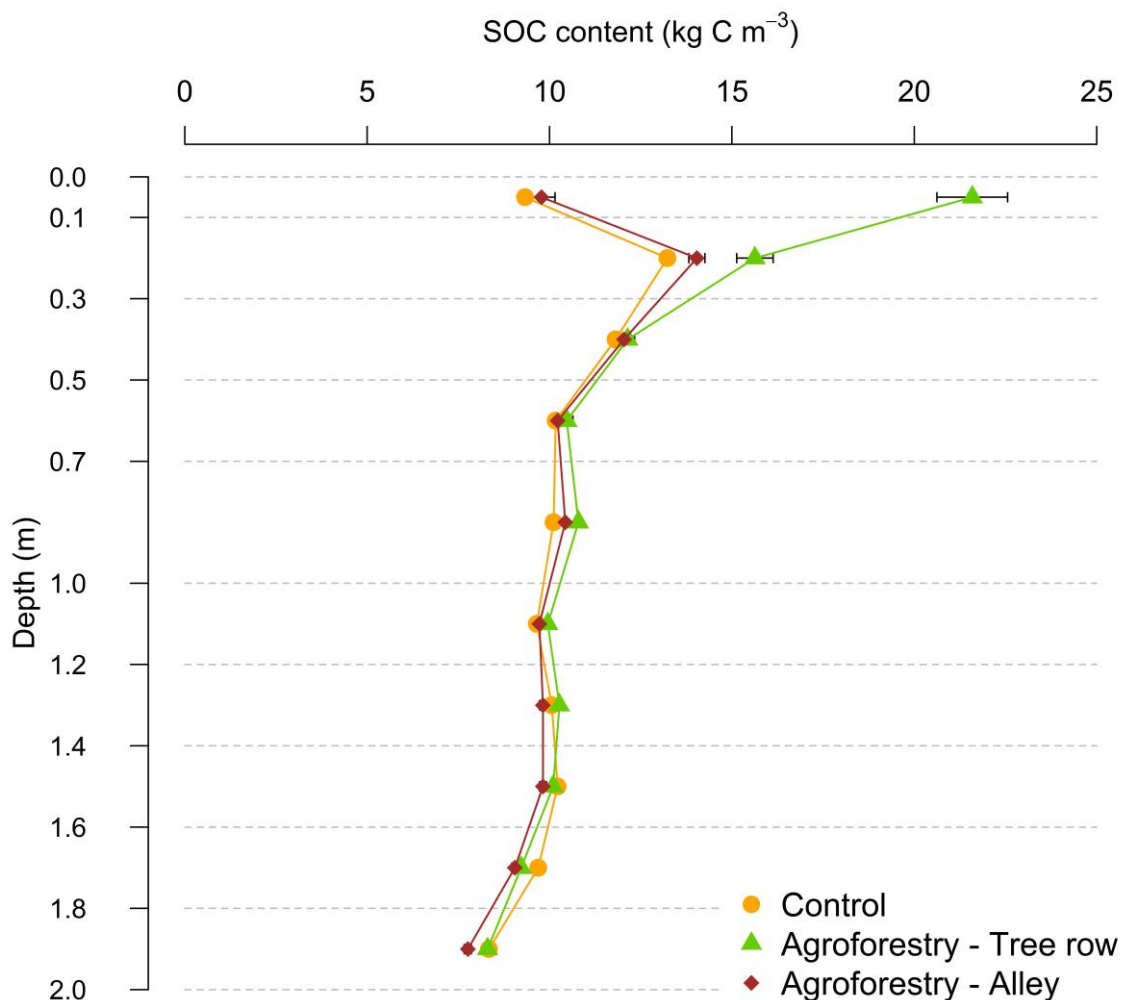
166 DBH: Diameter at Breast Height; ABG: aboveground; OC: organic carbon; HSOC: humified  
 167 soil organic carbon.

168

## 169 2.2 Organic carbon stocks

### 170 2.2.1 Soil organic carbon stocks

171 SOC data have been published in Cardinael *et al.*, (2015b) (Fig. 1). Briefly, soil cores were  
172 sampled down to 2 m depth in May 2013, 100 in the agroforestry plot, and 93 in the agricultural  
173 control plot. SOC concentrations, soil bulk densities, SOC stocks, and soil texture were  
174 measured for ten soil layers (0.0-0.1, 0.1-0.3, 0.3-0.5, 0.5-0.7, 0.7-1.0, 1.0-1.2, 1.2-1.4, 1.4-1.6,  
175 1.6-1.8, and 1.8-2.0 m). In the agroforestry plot, 40 soil cores were taken in the tree rows, while  
176 60 were sampled in the alleys at varying distances from the trees. Soil organic carbon stocks  
177 were quantified on an equivalent soil mass basis (Ellert and Bettany, 1995).



178

179 Fig. 1. Soil organic carbon content in both the agroforestry and agricultural control plot.

180 Associated errors are standard errors. N = 93 in the control, N = 40 in the agroforestry

181 tree row, N = 60 in the agroforestry alley. Data from Cardinael *et al.*, (2015b).

182

## 183 **2.2.2 Tree aboveground and stump carbon stocks**

184 Three hybrid walnuts were chopped down in 2012. The trunk circumference was measured  
185 every meter up to the maximum height of the tree to estimate its volume. The trunk biomass  
186 was estimated by multiplying the trunk volume by the wood density that was measured at 616  
187 kg m<sup>-3</sup> during a previous work at the same site (Talbot, 2011). Then, branches were cut, the  
188 stump was uprooted, and they were weighted separately. Samples were brought to the  
189 laboratory to determine the moisture content, which enabled calculation of the branches and the  
190 stump dry mass.

191

## 192 **2.3 Measurements of organic carbon inputs in the field**

### 193 **2.3.1 Carbon inputs from tree fine root mortality**

194 The tree fine root (diameter  $\leq 2$  mm) biomass was quantified and coupled with an estimate of  
195 the tree fine root turnover in order to predict the carbon input to the soil from the tree fine root  
196 mortality. A detailed description of the methods used to estimate the tree fine root biomass can  
197 be found in Cardinael *et al.*, (2015a). In March 2012, a 5 (length)  $\times$  1.5 (width)  $\times$  4 m (depth)  
198 pit was open in the agroforestry plot, perpendicular to the tree row, at the North of the trees.  
199 The tree fine root distribution was mapped down 4 m depth, and the tree fine root biomass was  
200 quantified in the tree row and in the alley. Only results concerning the first two meters of soil,  
201 among those obtained by Cardinael *et al.*, (2015a) will be used here.

202 In July 2012, sixteen minirhizotrons were installed in the agroforestry pit, at 0, 1, 2.5 and 4 m  
203 depth, and at two and five meters from the trees. The tree root growth and mortality was

204 monitored during one year using a scanner (CI-600 Root Growth Monitoring System, CID,  
205 USA), and analyzed using the WinRHIZO Tron software (Régent, Canada). A detailed  
206 description of the methods and of results used to estimate the tree fine root turnover can be  
207 found in Germon *et al.*, (2016).

208

### 209 **2.3.2 Tree litterfall**

210 In 2009, the crowns of two walnut trees were packed with a net in order to collect the leaf  
211 biomass from September to January. The same was done in 2012 with three other walnut trees.  
212 The leaf litter was then dried, weighted and analyzed for C to quantify the leaf carbon input per  
213 tree.

214

### 215 **2.3.3 Aboveground and belowground input from the crop**

216 Since the tree planting in 1995, the crop yield was measured 14 times (in 1995, 2000, 2002,  
217 2003, 2004, 2005, 2007, 2008, 2009, 2010, 2011, 2012, 2013, and 2014), while the wheat straw  
218 biomass and the total aboveground biomass were measured six times (in 2007, 2008, 2009,  
219 2011, 2012, and 2014) in both the control and the agroforestry plot (Dufour *et al.*, 2013), using  
220 sampling subplots of 1 m<sup>2</sup> each. In the control plot, five subplots have been sampled while in  
221 the agroforestry plot five transects have been sampled. Each transect was made of three  
222 subplots, 2 m North from the tree, 2 m South from the tree, and 6.5 m from the tree (middle of  
223 the alley). In March 2012, a 2 m deep pit was opened in the agricultural control plot (Prieto *et*  
224 *al.*, 2015), and the root biomass was quantified to the maximum rooting depth (1.5 m). The  
225 root:shoot ratio of durum wheat was measured in the control plot. We assumed that the crop  
226 root biomass turns out once a year, after the crop harvest.

227

### 228 **2.3.4 Above and belowground input from the tree row herbaceous vegetation**

229 As two types of herbaceous vegetation grow in the tree rows during the year, samples were  
 230 taken in summer and winter. In late June 2014, twelve subplots of 1 m<sup>2</sup> each were positioned  
 231 in the tree rows, around 4 walnut trees. In January 2015, six subplots of 1 m<sup>2</sup> each were  
 232 positioned in the tree rows, around 2 walnut trees. The middle of each subplot was located at 1  
 233 m, 2 m and 3 m, respectively, from the selected walnut tree. All the aboveground vegetation  
 234 was collected in each square. In the middle of each subplot, root biomass was sampled with a  
 235 cylindrical soil corer (inner diameter of 8 cm). Soil was taken at three soil layers, 0.0-0.1, 0.1-  
 236 0.3 and 0.3-0.5 m. In the laboratory, soil was gently washed with water through a 2 mm mesh  
 237 sieve, and roots were collected. Roots from the herbaceous vegetation were easily separated  
 238 manually from walnut roots, as they were soft and yellow compared to walnuts roots that were  
 239 black. After being sorted out from the soil and cleaned, the root biomass was dried at 40°C and  
 240 measured.

241

#### 242 **2.4 Carbon concentration measurements**

243 All organic carbon measurements were performed with a CHN elemental analyzer (Carlo Erba  
 244 NA 2000, Milan, Italy), after samples were oven-dried at 40°C for 48 hours (Table 2). Dry  
 245 biomasses (t DM ha<sup>-1</sup>) of each organic matter inputs were multiplied by their respective organic  
 246 carbon concentrations (mg C g<sup>-1</sup>) to calculate organic carbon stocks (t C ha<sup>-1</sup>).

247

248 **Table 2.** Organic carbon concentrations and C:N ratio of the different types of biomass.

Type of biomass	Organic C concentration (mg C g <sup>-1</sup> )	C:N	Number of replicates
Walnut trunk	445.7 ± 1.0	159.1 ± 25.2	3
Walnut branches	428.6 ± 1.7	62.2 ± 11.7	3
Wheat straw	433.2 ± 0.7	55.5 ± 2.1	5
Wheat root	351.4 ± 19	24.8 ± 2.1	8
Walnut leaf	449.4 ± 3.7	49.1 ± 0.4	3
Walnut fine root	437.0 ± 3.3	28.6 ± 3.4	8
Summer vegetation (ABG)	448.4 ± 1.9	37.8 ± 2.2	5
Summer vegetation (roots)	314.5 ± 8.3	33.8 ± 1.7	6

Winter vegetation (ABG)	447.7 ± 5.3	11.2 ± 0.4	3
Winter vegetation (roots)	397.4 ± 5.0	24.7 ± 0.7	3

249 The organic matter called “vegetation” stands for the herbaceous vegetation that grows in the  
 250 tree row. ABG: aboveground. Errors represent standard errors.

251

## 252 **2.5 General description of the CARBOSAF model**

### 253 **2.5.1 Organic carbon decomposition**

254 We adapted a model developed by Guenet et al. (2013) where total SOC is split in two pools,  
 255 the FOC and the humified soil organic carbon (HSOC) for each soil layer (Fig. 1a). Input to the  
 256 FOC pool comes from the plant litter and the distribution of this input within the profile is  
 257 assumed to depend upon depth from the surface ( $z$ ), distance from the tree ( $d$ ), and time ( $t$ ).  
 258 Equations describing inputs to the FOC pool ( $I_{t,z,d}$ ) at a given time, depth, and distance are  
 259 fully explained in the Results.

260

261 The FOC mineralisation is assumed to be governed by first order kinetics, being proportional  
 262 to the FOC pool, as given by:

$$263 \quad dec\_FOC_{t,z,d} = -k_{FOC} \times FOC_{t,z,d} \times f_{clay,z} \times f_{moist,z} \times f_{temp,z} \quad (1)$$

264 where  $FOC_{t,z,d}$  is the FOC carbon pool ( $\text{kg C m}^{-2}$ ) at a given time ( $t$ , in years), depth ( $z$ , in m)  
 265 and distance ( $d$ , in m), and  $k_{FOC}$  is its decomposition rate. The potential decomposition rates of  
 266 the different plant materials were assessed with a 16-week incubation experiment during a  
 267 companion study at the site (Prieto et al., 2016). The decomposition rate  $k_{FOC}$  was weighted by  
 268 the respective contribution of each type of plant litter as a function of the tree age, soil depth  
 269 and distance from the tree. The rate modifiers  $f_{clay,z}$ ,  $f_{moist,z}$  and  $f_{temp,z}$  are functions depending  
 270 respectively on the clay content, soil moisture and soil temperature at a given depth  $z$ , and range  
 271 between 0 and 1.

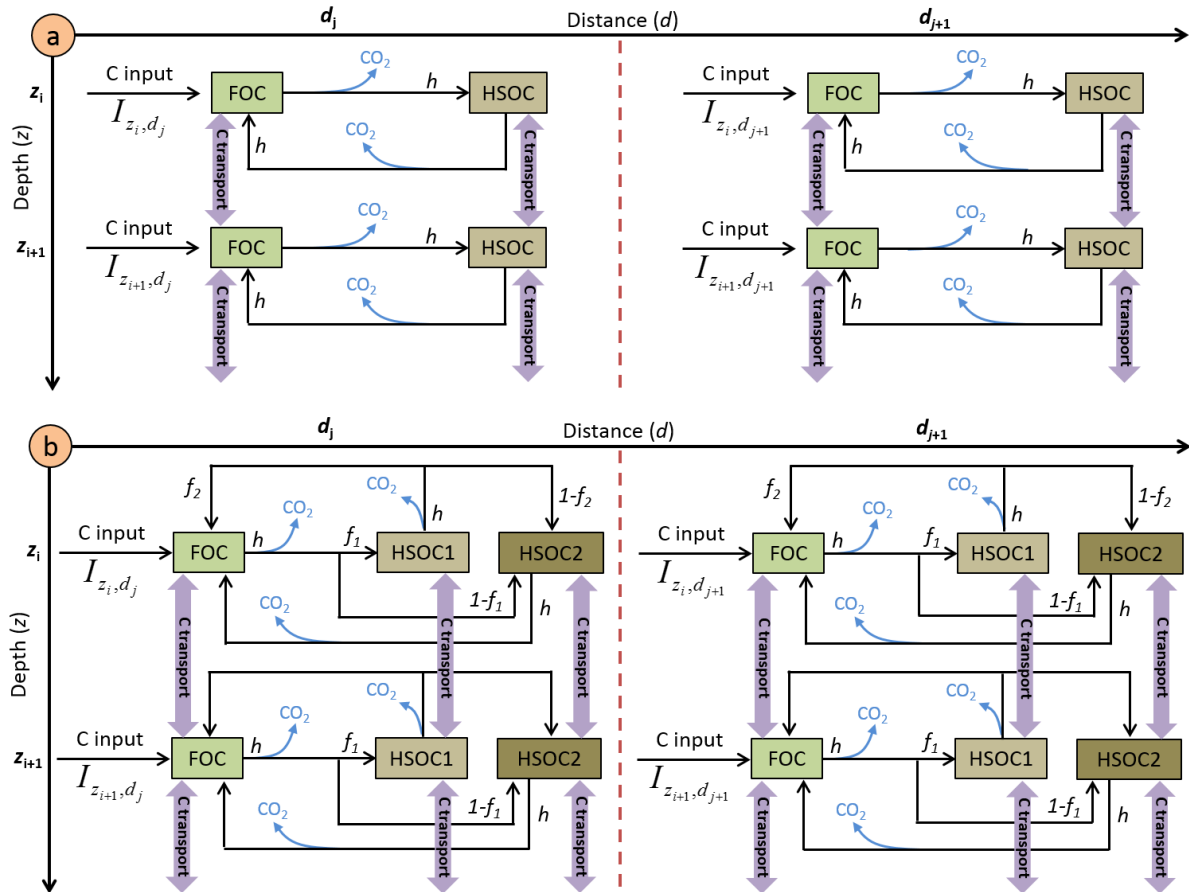
272

273 The  $f_{clay}$  function originated from the CENTURY model (Parton et al., 1987):

274 
$$f_{clay,z} = 1 - 0.75 \times Clay_z \quad (2)$$

275 where  $Clay_z$  is the clay fraction (ranging between 0 and 1) of the soil at a given depth  $z$ .

276



277

278 **Fig. 21.** Schematic representation of the pools and the fluxes of the (a) two pools model and (b)  
 279 three pools model.

280

281 The  $f_{moist,z}$  function originated from the meta-analysis of Moyano *et al.*, (2012) and is affected  
 282 by soil properties (clay content, SOC content). Briefly, the authors fitted linear models on 310  
 283 soil incubations to describe the effect of soil moisture on decomposition. Then, they normalized  
 284 such linear models between 0 and 1 to apply these functions to classical first order kinetics. All  
 285 details are described in Moyano *et al.*, (2012). To save computing time, we calculated  $f_{moist,z}$



286 only once using measured SOC stocks instead of using modelled SOC stocks and repeated the  
 287 calculation at each time step.

288

289 The temperature sensitivity of the soil respiration is expressed as  $Q_{10}$ :

$$290 \quad f_{temp,z} = Q_{10}^{\frac{temp_z - temp_{opt}}{10}} \quad (3)$$

291 with  $temp_z$  being the soil temperature in K at each soil depth  $z$  and  $temp_{opt}$  a parameter fixed to  
 292 304.15 K. The  $Q_{10}$  value was fixed to 2, a classical value used in models (Davidson and  
 293 Janssens, 2006).

294

295 Once the FOC is decomposed, a fraction is humified ( $h$ ) and another is respired as CO<sub>2</sub> ( $1-h$ )  
 296 (Fig. 21a) following equations (4) and (5).

$$297 \quad Humified\ FOC_{t,z,d} = h \times dec\_FOC_{t,z,d} \quad (4)$$

$$298 \quad Respired\ FOC_{t,z,d} = (1 - h) \times dec\_FOC_{t,z,d} \quad (5)$$

299

300 Two mathematical approaches are available in the model to describe the mineralisation of  
 301 HSOC: a first order kinetics, as given by Eq. (6) or an approach developed by Wutzler &  
 302 Reichstein, (2008) and by Guenet *et al.*, (2013) introducing the priming effect, i.e., the  
 303 mineralisation of HSOC depends on FOC availability, and given by Eq. (7):

$$304 \quad dec\_HSOC_{t,z,d} = -k_{HSOC,z} \times HSOC_{t,z,d} \times f_{moist,z} \times f_{temp,z} \quad (6)$$

$$305 \quad dec\_HSOC_{t,z,d} = -k_{HSOC,z} \times HSOC_{t,z,d} \times (1 - e^{-PE \times FOC_{t,z,d}}) \times f_{moist,z}$$

$$306 \quad \times f_{temp,z} \quad (7)$$

307 where  $HSOC_{t,z,d}$  is the humified SOC carbon pool at a given time ( $t$ , in years), depth ( $z$ , in m)  
 308 and distance ( $d$ , in m),  $k_{HSOC,z}$  is its decomposition rate (yr<sup>-1</sup>) at a given depth  $z$ , and  $PE$  is the  
 309 priming effect parameter. The parameters  $f_{moist,z}$  and  $f_{temp,z}$  are functions depending respectively  
 310 on soil moisture and soil temperature at a given depth  $z$ , and affecting the decomposition rate

311 of HSOC. They correspond to the moisture equation from Moyano *et al.*, (2012) and to Eq. (3),  
312 respectively. The decomposition rate  $k_{HSOC,z}$  was an exponential law depending on soil depth  
313 ( $z$ ) as shown by an incubation study (see paragraph *HSOC decomposition rate* further in the  
314 M&M):

$$315 \quad k_{HSOC,z} = a \times e^{-b \times z} \quad (8)$$

316 The  $b$  parameter of this equation represented the ratio of labile C/stable C within the HSOC  
317 pool. The effect of clay on HSOC decomposition was implicitly taken into account in this  
318 equation as clay content increased with soil depth.

319 A fraction of decomposed HSOC returns to the FOC assuming that part of the HSOC  
320 decomposition products is as labile as FOC ( $h$ ) and another is respired as CO<sub>2</sub> (Fig. 2+[a](#)) in the  
321 two pools model.

322

323 Finally, we also developed an alternative version of the model with three pools by splitting the  
324 HSOC pools into two pools with different turnover rates, HSOC2 being more stabilized than  
325 HSOC1 (Fig. 2+[b](#)). The non-respired decomposed FOC is split between HSOC1 and HSOC2  
326 following a parameter  $f_1$ . The non-respired decomposed HSOC1 is split between HSOC2 and  
327 FOC following a parameter  $f_2$  whereas non-respired decomposed HSOC2 is only redistributed  
328 into the FOC pools. The decomposition of HSOC1 and HSOC2 both follow the equation (8)  
329 but with different parameter values for  $a$ .

330

### 331 **2.5.2 Carbon transport mechanisms**

332 The transport of C between the different soil layers was represented by both advection and  
333 diffusion mechanisms (Elzein and Balesdent, 1995), which have been shown to usually describe  
334 well the C transport in soils (Bruun *et al.*, 2007; Guenet *et al.*, 2013). The advection represents  
335 the C transport due to the water infiltration in the soil, while the diffusion represents the C

336 transport due to the fauna activity. The same transport coefficients were applied to the two C  
337 pools, FOC and HSOC.

338

339 The advection is defined by:

$$340 \quad F_A = A \times C \quad (9)$$

341 where  $F_A$  is the flux of  $C$  transported downwards by advection, and  $A$  is the advection rate (mm  
342  $\text{yr}^{-1}$ ).

343

344 The diffusion is represented by the Fick's law:

$$345 \quad F_D = -D \times \frac{\partial^2 C}{\partial z^2} \quad (10)$$

346 where  $F_D$  is the flux of  $C$  transported downwards by diffusion,  $-D$  the diffusion coefficient ( $\text{cm}^2$   
347  $\text{yr}^{-1}$ ) and  $C$  the amount of carbon in the pool subject to transport (FOC or HSOC).

348

349 To represent the effect of soil tillage ( $z \leq 0.2$  m), we added another diffusion term using the  
350 Fick's law but with a value of  $D$  several orders of magnitude higher to represent the mixing due  
351 to tillage. It must be noted that no tillage effect on the decomposition was represented here  
352 because of the large unknowns on these aspects (Dimassi et al., 2013; Virto et al., 2012).

353

354 In this model, the flux of  $C$  transported downwards by the advection and diffusion ( $F_{AD}$ ) was  
355 represented as the sum of both mechanisms, following Elzein & Balesdent (1995):

$$356 \quad F_{AD} = F_A + F_D \quad (11)$$

357

358 The FOC and HSOC pools dynamics in the two pools model correspond to:

$$359 \quad \frac{\partial FOC_{t,z,d}}{\partial t} = I_{t,z,d} + \frac{\partial F_{AD}}{\partial z} + h \times dec\_HSOC_{t,z,d} - dec\_FOC_{t,z,d} \quad (12)$$

$$360 \quad \frac{\partial HSOC_{t,z,d}}{\partial t} = \frac{\partial F_{AD}}{\partial z} + h \times dec\_FOC_{t,z,d} - dec\_HSOC_{t,z,d} \quad (13)$$

361

362 Finally, the FOC, HSOC1 and HSOC2 pools dynamics in the three pools model correspond to:

$$363 \quad \frac{\partial FOC_{t,z,d}}{\partial t} = I_{t,z,d} + \frac{\partial F_{AD}}{\partial z} + h \times f_2 \times dec\_HSOC1_{t,z,d} + h \times dec\_HSOC2_{t,z,d}$$

$$364 \quad - dec\_FOC_{t,z,d} \quad (14)$$

$$365 \quad \frac{\partial HSOC1}{\partial t} = \frac{\partial F_{AD}}{\partial z} + h \times f_1 \times dec\_FOC_{t,z,d} - dec\_HSOC1_{t,z,d} \quad (15)$$

$$366 \quad \frac{\partial HSOC2}{\partial t} = \frac{\partial F_{AD}}{\partial z} + h \times (1 - f_1) \times dec\_FOC_{t,z,d} + h \times (1 - f_2) \times dec\_HSOC1_{t,z,d}$$

$$367 \quad - dec\_HSOC2_{t,z,d} \quad (16)$$

368

### 369 2.5.3 Depth dependence of HSOC potential decomposition rates

370 The shape of the function (i.e. the  $b$  parameter) describing the HSOC potential decomposition  
 371 rate (Eq. (8)) was determined by incubating soils from the control, the alley and the tree row,  
 372 and from different soil layers (0.0-0.1, 0.1-0.3, 0.7-1.0 and 1.6-1.8 m). Soils were sieved at 5  
 373 mm, and incubated during 44 days at 20°C at a water potential of -0.03 MPa. Evolved CO<sub>2</sub> was  
 374 measured using a micro-GC at 1, 3, 7, 14, 21, 28, 35, 44 days. The three first measurement  
 375 dates corresponded to a pre-incubation period and were not included in the analysis. For a given  
 376 depth, the cumulative mineralised SOC was expressed as a percentage of total SOC and was  
 377 plotted against the incubation time. The slopes represented the potential SOC mineralisation  
 378 rate at a given soil depth and location. The potential SOC mineralisation rates were then plotted  
 379 against soil depth (Fig. S1). We used the soil incubations to determine only the  $b$  parameter of  
 380 the curve: with such short term incubations, the SOC decomposition rate over the soil profile  
 381 is overestimated because the CO<sub>2</sub> measured during the incubations mainly originates from the  
 382 labile C pool. The  $a$  parameter was optimized following the procedure described further.

383

## 384 **2.6 Boundary conditions of the CARBOSAF model**

### 385 **2.6.1 Annual aggregates of soil temperature and soil moisture**

386 In April 2013, eight soil temperature and moisture sensors (Campbell CS 616 and Campbell  
387 107, respectively) were installed in the agroforestry plot at 0.3, 1.3, 2.8 and 4.0 m depth, and at  
388 2 and 5 m from the trees. Soil temperature and moisture were measured for 11 months.

389 The mean annual soil temperature in the agroforestry plot was described by the following  
390 equation:

$$391 \quad T = -0.89 \times z + 288.24 \quad (R^2 = 0.99) \quad (17)$$

392 where  $T$  is the soil temperature (K) and  $z$  is the soil depth (m).

393

394 The mean annual soil moisture was described with the following equation:

$$395 \quad \theta = 0.05 \times z + 0.28 \quad (R^2 = 0.99) \quad (18)$$

396 where  $\theta$  is the soil volumetric moisture ( $\text{cm cm}^{-3}$ ) and  $z$  is the soil depth (m).

397 Due to a lack of data in the agricultural plot, we assumed that the soil temperature and the soil  
398 moisture were the same in the agroforestry tree rows, alleys and in the control plot, but we  
399 further performed a sensitivity analysis of the model on these two parameters.

400

### 401 **2.6.2 Interpolation of tree growth**

402 The tree growth has been measured in the field since the establishment of the experiment. We  
403 used the diameter at breast height ( $DBH$ ) as a surrogate of the tree growth preferentially to the  
404 tree height as the field measurements were more accurate. Indeed,  $DBH$  is easier to measure  
405 than height, especially when trees are getting older. To describe the temporal dynamic of  $DBH$   
406 since the tree planting, a linear equation was fitted on the data.

407 Tree growth measurements enabled us to fit the following equation that was used in the model:

$$408 \quad DBH_t \begin{cases} 0.01, & t \leq 3 \\ 0.0157 \times t - 0.0391 & 3 < t \leq 20 \end{cases} \quad (R^2 = 0.997) \quad (19)$$

409 where  $DBH_t$  is the diameter at breast height (m) and  $t$  represents the time since tree planting  
410 (years).

411

### 412 **2.6.3 Change of tree litterfall over time**

413 For the five walnut trees where the leaf biomass was quantified,  $DBH$  was also measured. The  
414 ratio between the leaf biomass and  $DBH$  was then calculated for the five replicates. Total leaf  
415 biomass was  $8.96 \pm 1.45$  kg DM tree<sup>-1</sup> and the carbon concentration of walnut leaves was  $449.4$   
416  $\pm 3.7$  mg C g<sup>-1</sup> (Table 2). With a density of 110 trees ha<sup>-1</sup>, leaf litterfall was estimated at  $0.73 \pm$   
417  $0.06$  t C ha<sup>-1</sup> in 2012 and at the plot scale. The ratio between leaf biomass and  $DBH$  was  $0.0277$   
418  $\pm 0.0024$  t C tree<sup>-1</sup> m<sup>-1</sup> or  $3.05$  t C ha<sup>-1</sup> m<sup>-1</sup>. The following linear relationship was therefore used  
419 in the model to describe leaf litter C input with the tree growth:

$$420 \quad L_t = 3.05 \times DBH_t \quad (20)$$

421 where  $L_t$  is the leaf litter input (t C ha<sup>-1</sup>) at the year  $t$ , and  $DBH_t$  the diameter at breast height  
422 (m) the year  $t$ .

423

### 424 **2.6.4 Tree fine root C input from mortality**

425 In 2012, the measured tree fine root biomass was higher in the tree row than in the alley (Table  
426 S1). From 0 to 1 m distance from the tree (in the tree row), the tree fine root biomass was  
427 homogeneous and was  $1.01$  t C ha<sup>-1</sup> down 2 m depth.

428 In 2012 and in the alley, the tree fine root biomass ( $TFRB$ ) decreased with increasing distance  
429 from the tree and was represented by an exponential function:

$$430 \quad TFRB = \begin{cases} 1.01, & 0 \leq d \leq 1 \\ 1.29 \times e^{-0.28 \times d} & 1 < d \leq 6.5 \end{cases} \quad (R^2 = 0.90), \quad (21)$$

431 where  $TFRB$  represents tree fine root biomass down 2 m depth (t C ha<sup>-1</sup>), and  $d$  the distance  
 432 from the tree (m).

433

434 We considered a linear increase of  $TFRB$  with increasing  $DBH$ , and a linear regression was  
 435 performed between  $TFRB$  in 2012 and  $TFRB$  in 1996, the first year after planting (biomass  
 436 considered as negligible). The following linear relationship was used to simulate  $TFRB$  as a  
 437 function of tree growth:

$$438 \quad TFRB_{t,d} = \begin{cases} 3.69 \times DBH_t, & 0 \leq d \leq 1 \\ 4.70 \times DBH_t \times e^{-0.28 \times d}, & 1 < d \leq 6.5 \end{cases} \quad (22)$$

439 where  $TFRB_t$  represents the tree fine root biomass to 2 m depth (t C ha<sup>-1</sup>) at the year  $t$ ,  $DBH_t$  the  
 440 diameter at breast height (m) at the year  $t$ , and  $d$  the distance to the tree (m).

441

442 A changing distribution of tree fine roots within the soil profile was taken into account with  
 443 increasing distance to the tree. For this purpose, exponential functions ( $a \times e^{-b \times z}$ ) were  
 444 fitted in the alley every 0.5 m distance, and a linear regression was fitted between their  
 445 coefficients  $a$  and  $b$  and distance from the tree. However, the distribution of  $TFRB$  within the  
 446 soil profile and with the distance to the tree was considered constant with time.

447 A decreasing exponential function best represented the changing distribution of tree fine roots  
 448 within the soil profile with increasing distance to the tree:

$$449 \quad p_{TFRB,z,d} = \begin{cases} 13.92 \times e^{-1.39 \times z} & (R^2 = 0.68), & 0 \leq d \leq 1 \\ a \times e^{-b \times z}, & & 1 < d \leq 6.5 \end{cases} \quad (23)$$

450 and

$$451 \quad a = 10.31 - 1.15 \times d \quad (R^2 = 0.69) \quad (24)$$

$$452 \quad b = -1.10 + 0.19 \times d \quad (R^2 = 0.51) \quad (25)$$

453 Finally,

$$454 \quad p_{TFRB,z,d} = \begin{cases} 13.92 \times e^{-1.39 \times z}, & 0 \leq d \leq 1 \\ (10.31 - 1.15 \times d) \times e^{-(-1.10 + 0.19 \times d) \times z}, & 1 < d \leq 6.5 \end{cases} \quad (26)$$

455 where  $p_{TFRB,z,d}$  is the proportion (%) of the total tree fine root biomass ( $TFRB$ ) at a given depth  
456  $z$  (m), and at a distance  $d$  from the tree (m).

457

458 To finally estimate the tree fine root input due to the mortality,  $TFRB$  was multiplied by the  
459 measured root turnover. The tree fine root turnover ranged from 1.7 to 2.8  $\text{yr}^{-1}$  depending on  
460 fine root diameter, with an average turnover of 2.2  $\text{yr}^{-1}$  for fine roots  $\leq 2$  mm and to a depth of  
461 2 m (Germon et al., 2016).

462

### 463 **2.6.5 Aboveground and belowground input from the crop**

464 As there were more crop yield measurements (14) than straw biomass measurements (6), the  
465 effect of agroforestry on the crop yield with time was used as an estimate for change in the  
466 aboveground and belowground wheat biomass.

467 For this, the relative yield ( $Rel Y_{AF}$ ) in the agroforestry system was calculated for each year as  
468 the ratio between the agroforestry yield and the control yield ( $Y_C$ ).

469 The average annual crop yield in the control plot was  $Y_C = 3.79 \pm 0.40$  t DM  $\text{ha}^{-1}$  for the 14  
470 studied years. In the agroforestry plot, the average relative yield decreased linearly with time  
471 (increasing  $DBH$ ) and was described using the following linear equation (Fig. 32):

$$472 \quad Rel Y_{AF_t} = -93.33 \times DBH_t + 100 \quad (R^2 = 0.12, \quad p - value = 0.02) \quad (27)$$

473 where  $Rel Y_{AF_t}$  is the average relative crop yield (%) in the agroforestry plot compared to the  
474 control plot at year  $t$ , and  $DBH_t$  is the diameter at breast height (m) at year  $t$ .

475

476 The variation of crop yield with distance from the trees was described with a quadratic equation  
477 (Fig. 2). But as we aimed to predict SOC stocks up to 6.5 m distance from the trees (middle of  
478 the alley), a linear increase of crop yield with increasing distance from the tree gave similar

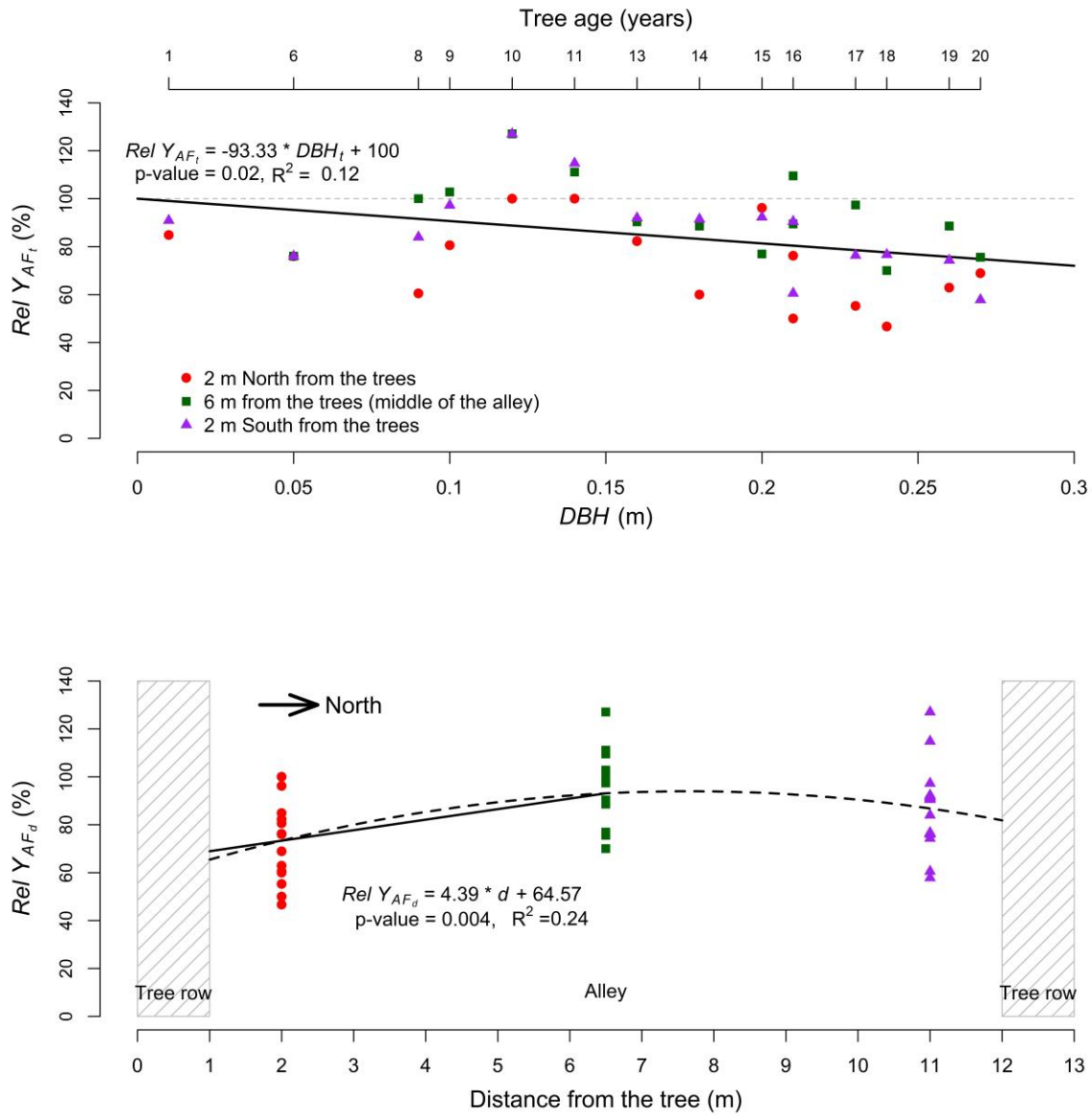


479 results as the quadratic equation over the 6.5 m distance and was more parsimonious:

480  $Rel Y_{AF_d} = 4.39 \times d + 64.57 \quad (R^2 = 0.24), \quad 1 < d \leq 6.5 \quad (28)$

481 where  $Rel Y_{AF_d}$  is the relative crop yield (%) in the agroforestry plot at a distance  $d$  (m) from

482 the tree compared to the control plot.



483  
 484 **Fig. 32.** Top: Relative yield ( $Rel Y_{AF_t}$ ) in the agroforestry plot compared to the control plot as  
 485 a function of tree growth, represented by the diameter at breast height ( $DBH$ ) at year  $t$ . Bottom:  
 486 Relative yield ( $Y_{AF_t,d}$ ) as a function of the distance from the tree.

487

488 Finally, the crop yield in the agroforestry plot was modeled as follows:

$$489 \quad Y_{AF,t,d} = Rel Y_{AF_t} \times Y_C \times Rel Y_{AF_d} \quad (R^2 = 0.19), \quad 1 < d \leq 6.5 \quad (29)$$

490 where  $Y_{AF,t,d}$  is the crop yield (t DM ha<sup>-1</sup>) in the agroforestry plot at the year  $t$  and at a distance  
491  $d$  (m) from the tree. Because three linear equations were used to describe the crop yield in the  
492 agroforestry plot, errors were accumulated and we finally came up with a standard  
493 underestimation of the crop yield in the agroforestry plot that we corrected by multiplying our  
494 equation by 1.2.

495

496 The ratio between the straw biomass and the crop yield was calculated as the average of the six  
497 measurements, and was considered constant with time. This ratio was used to convert crop yield  
498 into straw biomass. In the agroforestry plot, the carbon input to the soil from the aboveground  
499 crop biomass was:

$$500 \quad ABC_{crop,t,d} = Y_{AF,t,d} \times (straw \ biomass: \ crop \ yield) \times C_{straw} \times (1 - export) \quad (30)$$

501 where  $ABC_{crop,t,d}$  is the aboveground carbon input from the crop (t C ha<sup>-1</sup>) at the year  $t$  and  
502 distance  $d$  from the tree,  $Y_{AF,t,d}$  is the agroforestry crop yield. The average ratio between the  
503 straw biomass (t DM ha<sup>-1</sup>) and the crop yield (t DM ha<sup>-1</sup>) equaled  $1.03 \pm 0.11$  (n=6). The wheat  
504 straw was exported out of the field after the harvest, but it was estimated that 25% of the straw  
505 biomass was left on the soil, thus  $export=0.75$ . In the control plot,  $Y_{AF,t,d}$  was replaced by  $Y_C$ .

506 To estimate fine root biomass of the crop, we hypothesized that the root:shoot ratio of the durum  
507 wheat was the same in both the agroforestry and agricultural plot, in the absence of any  
508 published data on the matter. In the agroforestry plot, the belowground crop biomass was  
509 represented by:

$$510 \quad BEC_{crop,t,d} = Y_{AF,t,d} \times (shoot: \ crop \ yield) \times (root: \ shoot) \times C_{root} \quad (31)$$

511 where  $BEC_{crop,t,d}$  is the belowground crop biomass (t C ha<sup>-1</sup>) at the year  $t$  and at a distance  $d$   
512 from the tree,  $Y_{AF,t,d}$  is the agroforestry crop yield. The average ratio between the total crop

513 aboveground biomass (*shoot*) and the crop yield equaled  $2.45 \pm 0.15$  (n=6). In 2012, total fine  
 514 root biomass was  $2.29 \pm 0.32$  t C ha<sup>-1</sup> in the control (Table 3).

515

516 **Table 3.** Wheat fine root biomass in the agricultural control plot in 2012.

Soil depth (m)	Wheat fine root biomass	
	(kg C m <sup>-3</sup> )	(t C ha <sup>-1</sup> )
0.0-0.1	0.48 ± 0.05	0.48 ± 0.05
0.1-0.3	0.34 ± 0.04	0.69 ± 0.09
0.3-0.5	0.22 ± 0.04	0.44 ± 0.08
0.5-1.0	0.10 ± 0.04	0.52 ± 0.20
1.0-1.5	0.03 ± 0.04	0.17 ± 0.19
Total	-	2.29 ± 0.32

517 Errors represent standard errors.

518

519 Therefore, the wheat *root:shoot* ratio equaled  $0.79 \pm 0.12$  (n=1). The carbon concentration of  
 520 wheat root was  $C_{root} = 35.14 \pm 1.90$  mg C g<sup>-1</sup>. In the control plot,  $Y_{AF,t,d}$  was replaced by  $Y_C$ .

521

522 In 2012, no wheat roots were observed below 1.5 m, and root biomass decreased exponentially  
 523 with increasing depth (Table 3). The distribution of crop roots within the soil profile was  
 524 described as follows:

$$525 \quad p_{CRBc,z} = \begin{cases} 26.44 \times e^{-2.59 \times z} & (R^2 = 0.99), & z \leq 1.5 \\ 0, & z > 1.5 \end{cases} \quad (32)$$

526 where  $p_{CRBc,z}$  is the proportion (%) of total crop root biomass in the control plot at a given  
 527 depth  $z$  (m).

528 Since the same maximum rooting depth of the crop was observed in the agroforestry plot and  
 529 in the control plot, we inferred that the wheat root distribution within the soil profile was not  
 530 modified by agroforestry, but only its biomass. The crop root turnover was assumed to be 1 yr<sup>-1</sup>,  
 531 root mortality occurring mainly after crop harvest.

532

533

## 534 2.6.6 Aboveground and belowground input from herbaceous vegetation in the tree rows

535 The distance from the trees had no effect on the above and belowground biomass of the  
536 herbaceous vegetation (data not shown), therefore average values are presented. The summer  
537 aboveground biomass was almost three times higher than in winter, whereas the belowground  
538 biomass was two times higher (Table 4). The total aboveground carbon input was  $2.13 \pm 0.14$  t  
539  $\text{C ha}^{-1} \text{ yr}^{-1}$  and the total belowground carbon input was  $0.74 \pm 0.05$  t  $\text{C ha}^{-1} \text{ yr}^{-1}$  to 0.5 m depth.

540

541 **Table 4.** Aboveground and belowground biomass of the herbaceous vegetation in the tree rows.

	Soil depth (m)	Herbaceous biomass (t C ha <sup>-1</sup> )	
		Summer	Winter
Aboveground	-	$1.57 \pm 0.11$	$0.56 \pm 0.09$
Belowground	0.0-0.1	$0.22 \pm 0.03$	$0.17 \pm 0.01$
	0.1-0.3	$0.16 \pm 0.02$	$0.06 \pm 0.01$
	0.3-0.5	$0.09 \pm 0.04$	$0.04 \pm 0.01$
	Total	$0.46 \pm 0.04$	$0.27 \pm 0.02$

542 Errors represent standard errors.

543

544 The belowground carbon input from the tree row vegetation ( $BEC_{veg,z}$ , t C ha<sup>-1</sup>) at a given depth  
545  $z$  (m) was described by the following equation:

$$546 \quad BEC_{veg,z} = \begin{cases} 0.44 \times e^{-3.12 \times z}, & z \leq 1.5 \\ 0, & z > 1.5 \end{cases} \quad (33)$$

547 We assumed for simplification that the aboveground and belowground biomasses of the  
548 herbaceous vegetation in the tree row were constant over time.

549

## 550 2.7 Optimization procedure

551 Depending on the model variant, four to five parameters were optimized with a **Bayesian**  
552 **gradient based** statistical method (Santaren et al., 2007; Tarantola, 1987, 2005) using measured  
553 SOC stocks from the control plot only. These parameters were  $A$ , the advection rate,  $D$ , the

554 diffusion coefficient,  $h$  the humification yield,  $a$  the coefficient of the  $k_{HSOC}$  rate from Eq. (10),  
 555 and  $PE$  the priming coefficient. These four or five parameters were calibrated so that  
 556 equilibrium SOC stocks, i.e. after 5000 years of simulation, equaled SOC stocks of the control  
 557 plot in 2013. The associated uncertainty was estimated with the 93 soil cores sampled in the  
 558 control plot (see section 2.2.1). Due to a lack of relevant data, we assumed that the climate and  
 559 the land use were the same for the last 5000 years, and that SOC stocks in the control plot were  
 560 at equilibrium at the time of measurement. Therefore, SOC stocks at the end of the 5000 years  
 561 of simulation equaled SOC stocks in the control plot. Three different calibrations were  
 562 performed, corresponding to the three ~~different-models~~ variants that were used: one calibration  
 563 with the two pools model without the priming effect, one calibration with the two pools model  
 564 with the priming effect, and one calibration with the three pools model.

565 Each model variant was fitted to the control SOC stocks data using a ~~Bayesian~~ curve fitting  
 566 method described in Tarantola (1987), after a conversion from SOC stocks in  $\text{kg C m}^{-2}$  to SOC  
 567 stocks in  $\text{kg m}^{-3}$  due to the different soil layers' thickness. We aimed to find a parameter set  
 568 that minimizes the distance between model outputs and the corresponding observations,  
 569 considering model and data uncertainties, and ~~prior-starting parameter~~ information on  
 570 parameters. With the assumption of Gaussian errors for both the observations and the ~~prior~~  
 571 starting parameters, the optimal parameter set corresponds to the minimum of the cost function  
 572  $J(\mathbf{x})$ :

$$573 \quad J(\mathbf{x}) = 0.5 \times [(\mathbf{y} - \mathbf{H}(\mathbf{x}))^t \times \mathbf{R}^{-1} \times (\mathbf{y} - \mathbf{H}(\mathbf{x})) + (\mathbf{x} - \mathbf{x}_b)^t \times \mathbf{P}_b^{-1} \times (\mathbf{x} - \mathbf{x}_b)] \quad (34)$$

574 that contains both the mismatch between modelled and observed SOC stock and the mismatch  
 575 between a ~~prior-starting~~ and optimized parameters.  $\mathbf{x}$  is the vector of unknown parameters,  $\mathbf{x}_b$   
 576 the vector of a ~~prior-starting~~ parameter values fixed for each optimization procedures,  $\mathbf{H}()$  the  
 577 model and  $\mathbf{y}$  the vector of observations. The covariance matrices  $\mathbf{P}_b$  and  $\mathbf{R}$  describe a priori  
 578 uncertainties on parameters, and observations, respectively. Both matrices are diagonal as we

579 suppose the observation uncertainties and the parameter uncertainties to be independent. The  
580 covariance matrices  $P_b$  are presented in Table S2. To determine an optimal set of parameters  
581 which minimizes  $J(\mathbf{x})$ , we used the BFGS gradient-based algorithm (Tarantola, 1987). For each  
582 model variant, we performed 30 optimizations starting with different starting parameter prior  
583 values to check that the results did not correspond to a local minimum. As the BFGS algorithm  
584 does not directly calculate the variance of posteriors, they were quantified using the curvature  
585 cost function at its minimum once it was reached (Santaren et al., 2007).

586

## 587 **2.8 Comparison of models**

588 Model predictions with and without priming effect were compared calculating the coefficients  
589 of determination, root mean square errors (RMSE) and Bayesian information criteria (BIC).

$$590 \quad RMSE = \sqrt{\frac{1}{N} \sum_{i=1}^N (x_i - \bar{x})^2} \quad (35)$$

591 where  $i$  is the number of observations (1 to  $N$ ),  $x_i$  is the predicted value and  $\bar{x}$  is the mean  
592 observed value.

$$593 \quad BIC = k \times \ln(N) - 2 \times \ln(\hat{L}) \quad (36)$$

594 where  $N$  is the number of observations,  $k$  is the number of model parameters, and  $\hat{L}$  is the  
595 maximized value of the likelihood function of the model (Schwarz, 1978).

596

597 The model was run at a yearly time step using mean annual soil temperature and moisture and  
598 annual C inputs to the soil. In the agroforestry, the model was run from the ground (0 m) to 2  
599 m depth, and from the tree (0 m) to 6.5 m from the tree (middle of the alley). The model was  
600 applied separately across locations of a tree-distance gradient having varying OC inputs, each  
601 soil column was considered independent from another. SOC pools were initialized after a spin-

602 up of 5000 years in the control plot. At  $t_0$ , SOC stocks in the agroforestry plot therefore equaled  
603 SOC stocks of the control plot. The model was then run from  $t_0$  to  $t_{18}$  (years) after tree planting.  
604 The spatial resolution was 0.1 m both vertically and horizontally. The model was developed  
605 using R 3.1.1 (R Development Core Team, 2013). Partial-differential equations were solved  
606 using the R package *deSolve* and the *ode.ID* method (Soetaert et al., 2010).

607

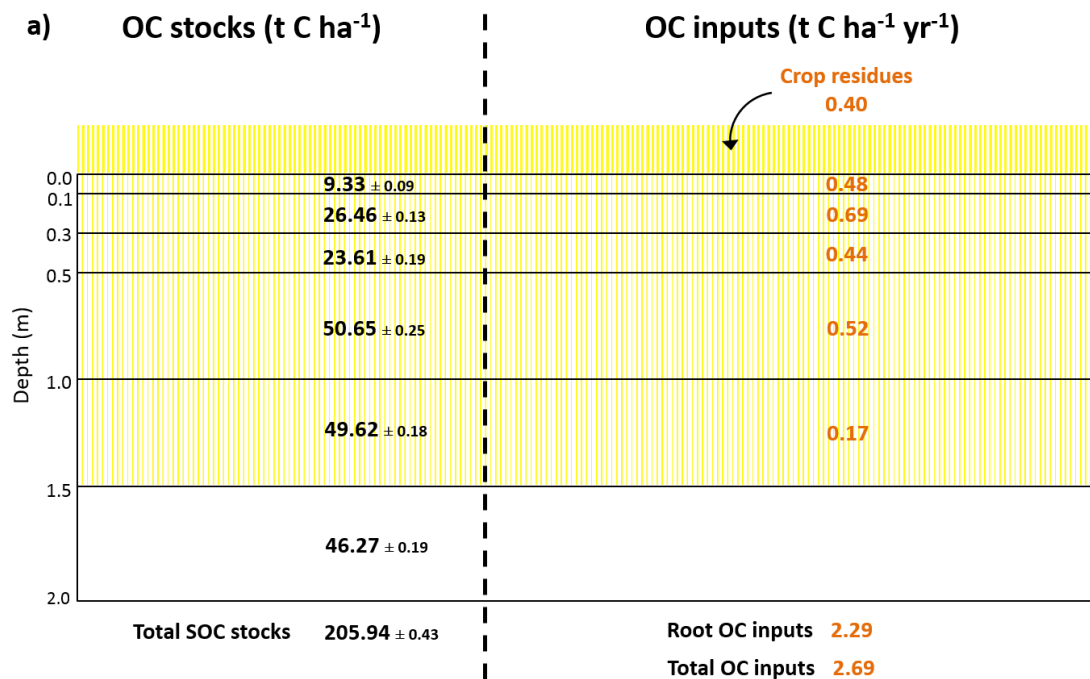
## 608 **3 Results**

### 609 **3.1 Organic carbon inputs and SOC stocks: a synthesis from field measurements**

610 In the alleys of the 18-year-old agroforestry system, measured organic carbon (OC) inputs from  
611 the crop residues and roots were reduced compared to the control plot due a lower crop yield  
612 (Fig. 43). This reduction in crop OC inputs was offset by OC inputs from the tree roots and tree  
613 litterfall. Total root OC inputs in the alleys (crop + tree roots) and in the control plot (crop roots)  
614 were very similar, respectively 2.43 and 2.29 t C ha<sup>-1</sup> yr<sup>-1</sup>. Alleys received 0.60 t C ha<sup>-1</sup> yr<sup>-1</sup>  
615 more of total aboveground biomass (crop residues + tree litterfall) than the control, which was  
616 added to the plough layer. Tree rows received 2.35 t C ha<sup>-1</sup> yr<sup>-1</sup> more C inputs in the first 0.3 m  
617 of soil compared to the control plot, mainly from the herbaceous vegetation. Down the whole  
618 soil profile, tree rows received two times more OC inputs compared to the control plot (Fig.  
619 43), and 65% more than alleys. Overall, the agroforestry plot had 41% more OC inputs to the  
620 soil than the control plot to 2 m depth (3.80 t C ha<sup>-1</sup> yr<sup>-1</sup> compared to 2.69 t C ha<sup>-1</sup> yr<sup>-1</sup>). In the  
621 agroforestry plot, the largest aboveground OC input to the soil comes from the herbaceous  
622 vegetation, and not from the trees. In the control plot, 85% of OC inputs are wheat root litters.  
623 In the agroforestry plot, root inputs represent 71% of OC inputs in the alleys, and 50% in the  
624 tree rows.

625 In the first 0.3 m of soil, SOC stocks were significantly higher in the alleys than in the control  
626 plot, but the difference was small ( $2.1 \pm 0.6$  t C ha<sup>-1</sup>). Between 0.3 and 1.0 m, the difference of

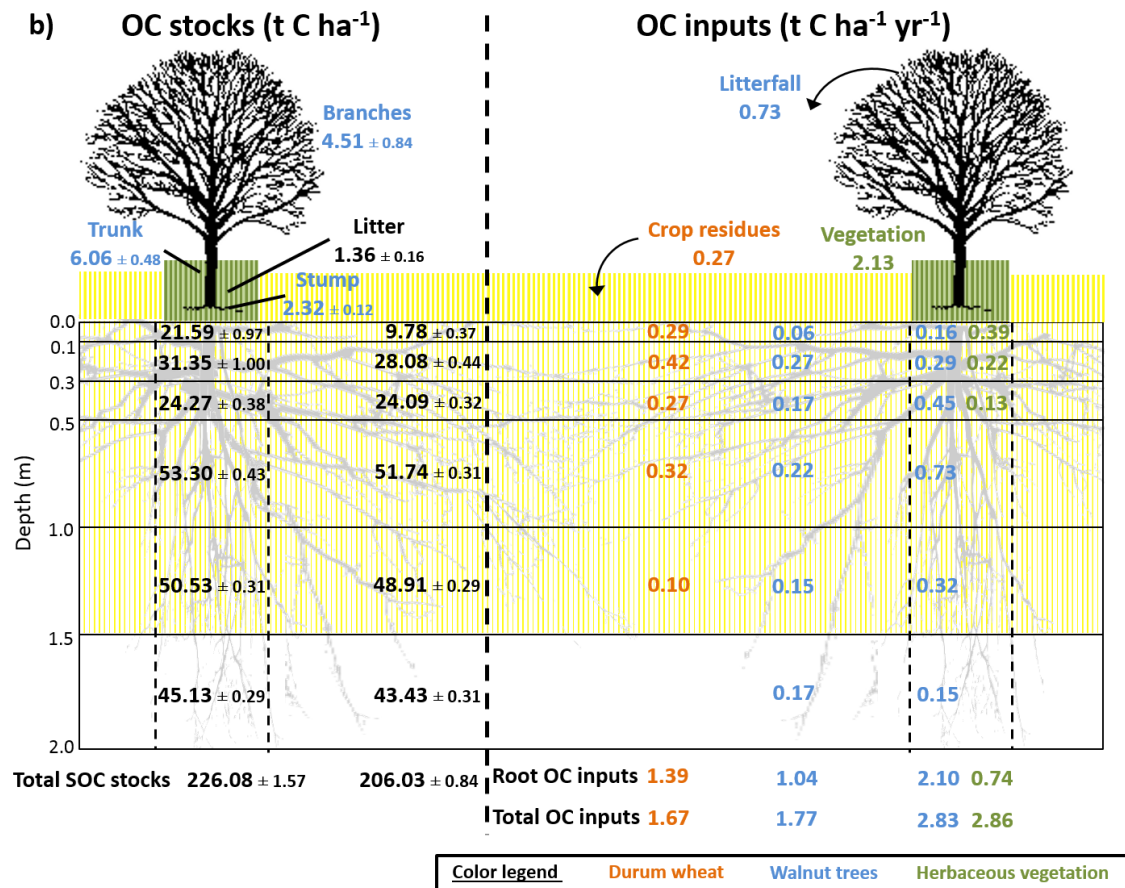
627 SOC stocks was smaller but still significant. However, between 1 and 2 m depth, SOC stocks  
 628 were significantly lower in the alleys than in the control. As a consequence, there was no  
 629 significant difference of total SOC stocks between the two locations down the whole soil  
 630 profile. In the tree rows, topsoil organic carbon stocks (0.0-0.3 m) were much higher than in  
 631 the control ( $+ 17.0 \pm 1.4 \text{ t C ha}^{-1}$ ). This positive difference of SOC stocks decreased with depth  
 632 but remained significantly positive down 1.5 m depth. The opposite was observed between 1.5  
 633 and 2.0 m depth. Delta of total SOC stocks between the tree rows and the control plot was  $20.1$   
 634  $\pm 1.6 \text{ t C ha}^{-1}$ . At the plot scale, total SOC stocks were significantly higher in the agroforestry  
 635 plot compared to the control plot down 2 m depth ( $+ 3.3 \pm 0.9 \text{ t C ha}^{-1}$ ).



636

637





638

639 **Fig. 43.** Measured soil organic carbon stocks and organic carbon inputs to the soil a) in the  
 640 agricultural control plot, b) in the 18-year-old agroforestry plot. Associated errors are  
 641 standard errors. Values are expressed per hectare of land type (control, alley, tree row).  
 642 To get the values per hectare of agroforestry, data from alley and tree row have to be  
 643 weighted by their respective surface area (i.e., 84% and 16%, respectively) and then  
 644 added up. OC: organic carbon; SOC: soil organic carbon. SOC stocks data are issued  
 645 from Cardinael *et al.*, (2015a), data of tree root OC inputs are combined from Cardinael  
 646 *et al.*, (2015b) and from Germon *et al.*, (2016).

647

### 648 3.2 HSOC decomposition rate

649 The soil incubation experiment showed that the HSOC mineralization rate decreased  
 650 exponentially with depth (Fig. S1) and could be described with:

651 
$$k_{HSOC,z} = 6.114 \times e^{-1.37 \times z} \quad (R^2 = 0.76) \quad (37)$$

652 where  $z$  is the soil depth (m), and where the  $a$  ( $\text{yr}^{-1}$ ) coefficient ( $a = 6.114$ ) was further optimized

653 (Table 5).

654

655 **Table 5.** Summary of optimized model parameters.

Model parameter	Meaning	Prior Starting parameter range (log)*	Posterior values $\pm$ variance (prior starting parameter values)		
			2 pools - without <i>PE</i>	2 pools - with <i>PE</i>	3 pools – without <i>PE</i>
<i>a</i>	coefficient from Eq. (8) of the HSOC decomposition ( $\text{yr}^{-1}$ )	<del>3.65e-6-12.52-1.29</del>	$0.01\text{e}^{-2} \pm <10^{-4}$ ( $0.01\text{e}^{-2}$ )	$0.01\text{e}^{-2} \pm <10^{-4}$ ( $0.01\text{e}^{-2}$ )	-
<i>a</i> <sub>1</sub>	coefficient from Eq. (8) of the HSOC1 decomposition ( $\text{yr}^{-1}$ )	<del>3.65e-6-12.52-1.29</del>	-	-	$0.01\text{e}^{-2} \pm <10^{-4}$ ( $0.01\text{e}^{-2}$ )
<i>a</i> <sub>2</sub>	coefficient from Eq. (8) of the HSOC2 decomposition ( $\text{yr}^{-1}$ )	<del>3.65e-6-12.52-1.29</del>	-	-	$0.83\text{e}^{-2} \pm 0.17\text{e}^{-2}$ ( $0.83\text{e}^{-2}$ )
<i>D</i>	diffusion coefficient ( $\text{cm}^2 \text{yr}^{-1}$ )	<del>1e-6-1-13.82-0</del>	$4.62\text{e}^{-4} \pm 5.95\text{e}^{-4}$ ( $9.64\text{e}^{-4}$ )	$5.63\text{e}^{-4} \pm 1.42\text{e}^{-4}$ ( $9.01\text{e}^{-4}$ )	$5.24\text{e}^{-4} \pm 7.62\text{e}^{-4}$ ( $9.64\text{e}^{-4}$ )
<i>A</i>	advection rate ( $\text{mm yr}^{-1}$ )	<del>1e-6-1-13.82-0</del>	$21.25\text{e}^{-4} \pm 5.02\text{e}^{-4}$ ( $8.54\text{e}^{-4}$ )	$6.63\text{e}^{-4} \pm 2.38\text{e}^{-4}$ ( $4.27\text{e}^{-4}$ )	$21.60\text{e}^{-4} \pm 2.24\text{e}^{-4}$ ( $8.54\text{e}^{-4}$ )
<i>h</i>	humification yield	<del>0.01-1-4.61-0</del>	$0.32 \pm <10^{-4}$ (0.34)	$0.25 \pm 1.00\text{e}^{-4}$ (0.13)	$0.34 \pm 0.03$ (0.34)
<i>PE</i>	priming coefficient	<del>0.1-160-2.30-5.08</del>	-	$9.66 \pm 1.49$ (102.95)	-
<i>f</i> <sub>1</sub>	fraction of decomposed FOC entering the HSOC1 pool	0-1	-	-	$0.99 \pm 0.18$ (0.86)
<i>f</i> <sub>2</sub>	fraction of decomposed HSOC1 entering the FOC pool	0-1	-	-	$0.94 \pm 1.10\text{e}^{-3}$ (0.80)

656 The prior starting parameter range represents the range in which prior starting parameter values were sampled for the 30 optimizations per model  
657 variant. The prior starting parameter values presented in brackets in the posterior column represent the prior starting parameter values that  
658 minimized the  $\mathbf{J}(\mathbf{x})$  value (Eq. (34)). ~~\*Except for  $f_1$  and  $f_2$ .~~  
659

## 660 3.3 Modeling results

### 661 3.3.1 Optimized parameters and correlation matrix

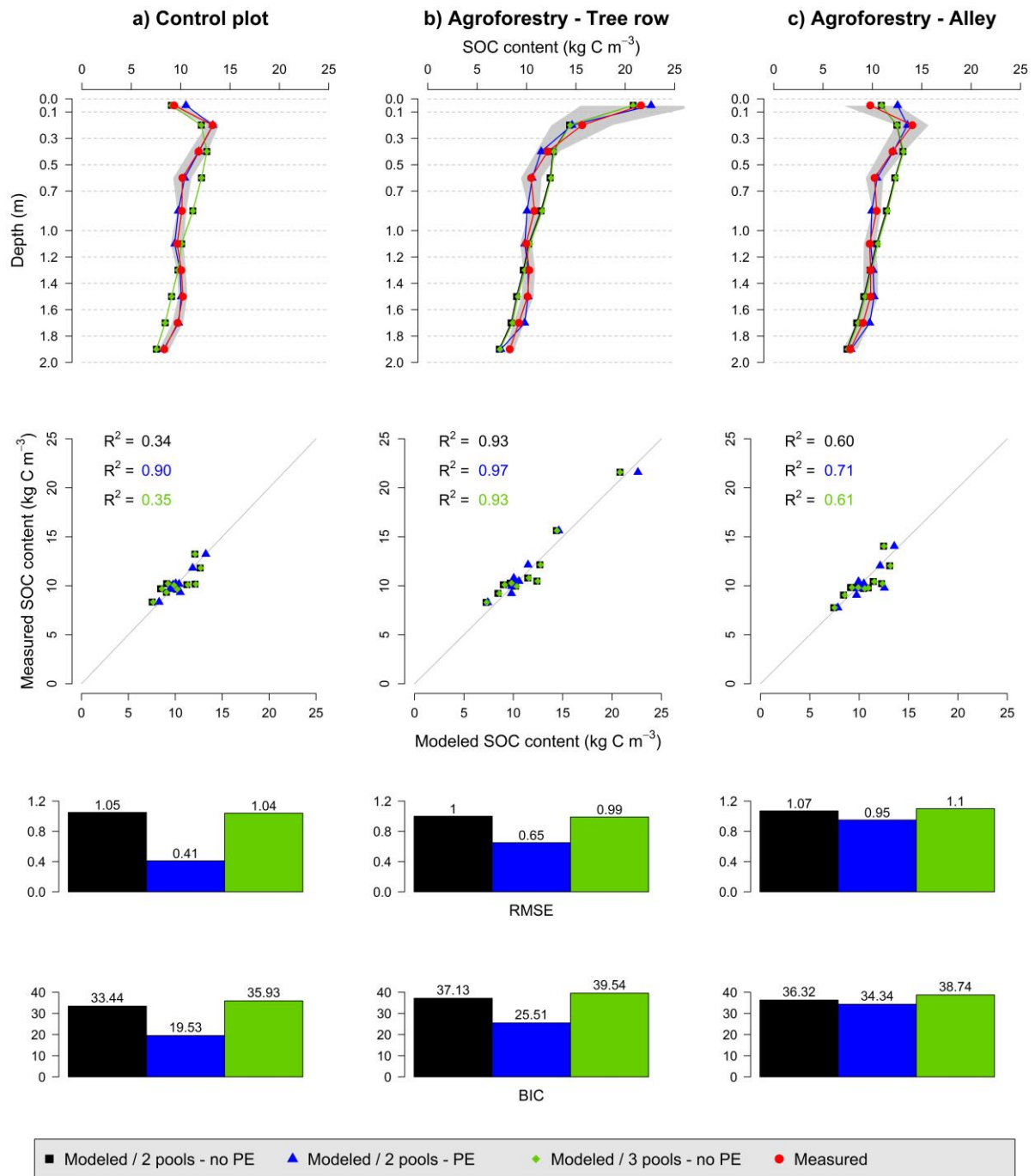
662 The optimized parameters and their ~~prior-starting parameter~~ modes are presented in Table 5.  
663 For the two pools model without priming effect, the most important correlation was observed  
664 between  $h$  and  $A$  which control the humification and the transport by advection. Concerning the  
665 two pools model with priming effect, the most important correlations were observed between  
666  $h$  and  $PE$  which controls the effect of the FOC on HSOC decomposition, and between  $h$  and  $A$ .  
667  $A$  and  $PE$  were also positively correlated (Fig. S2). For the three pools model,  $f_1$  and  $f_2$  were by  
668 definition negatively correlated, but  $f_2$  and  $A$  were also correlated. Considering the method used  
669 to optimize the parameters, these important correlation factors hinder the presentation of the  
670 model output within an envelope. Therefore, we presented the model results using the optimized  
671 parameter without any envelope.

672

### 673 3.3.2 Modeled SOC stocks

674 As a reminder, SOC stocks of the agroforestry plot were not part of model calibration (that used  
675 the control plot only) but were used here for validation. Observed SOC stocks were not well  
676 represented by the two pools model without priming effect, with RMSE ranging from 1.00 to  
677 1.07 kg C m<sup>-3</sup> (Fig. 54, Table S32). The model performed better when the priming effect was  
678 taken into account, with RMSE ranging from 0.41 to 0.95 kg C m<sup>-3</sup>, and the SOC profile was  
679 well described. The representation of SOC stocks was not improved by the inclusion of a third  
680 C pool in the model. Overall, the two pools model with priming effect was the best one, as  
681 shown by the BICs (Fig. 54, Table S32). For all models, SOC stocks below 1 m depth were  
682 better described than above SOC stocks (Table S32). The spatial distribution of SOC stocks  
683 and of additional SOC storage was also well described (Fig. 65), with a very high additional  
684 SOC storage in the topsoil layer in the tree row. Most modeled SOC storage in the agroforestry

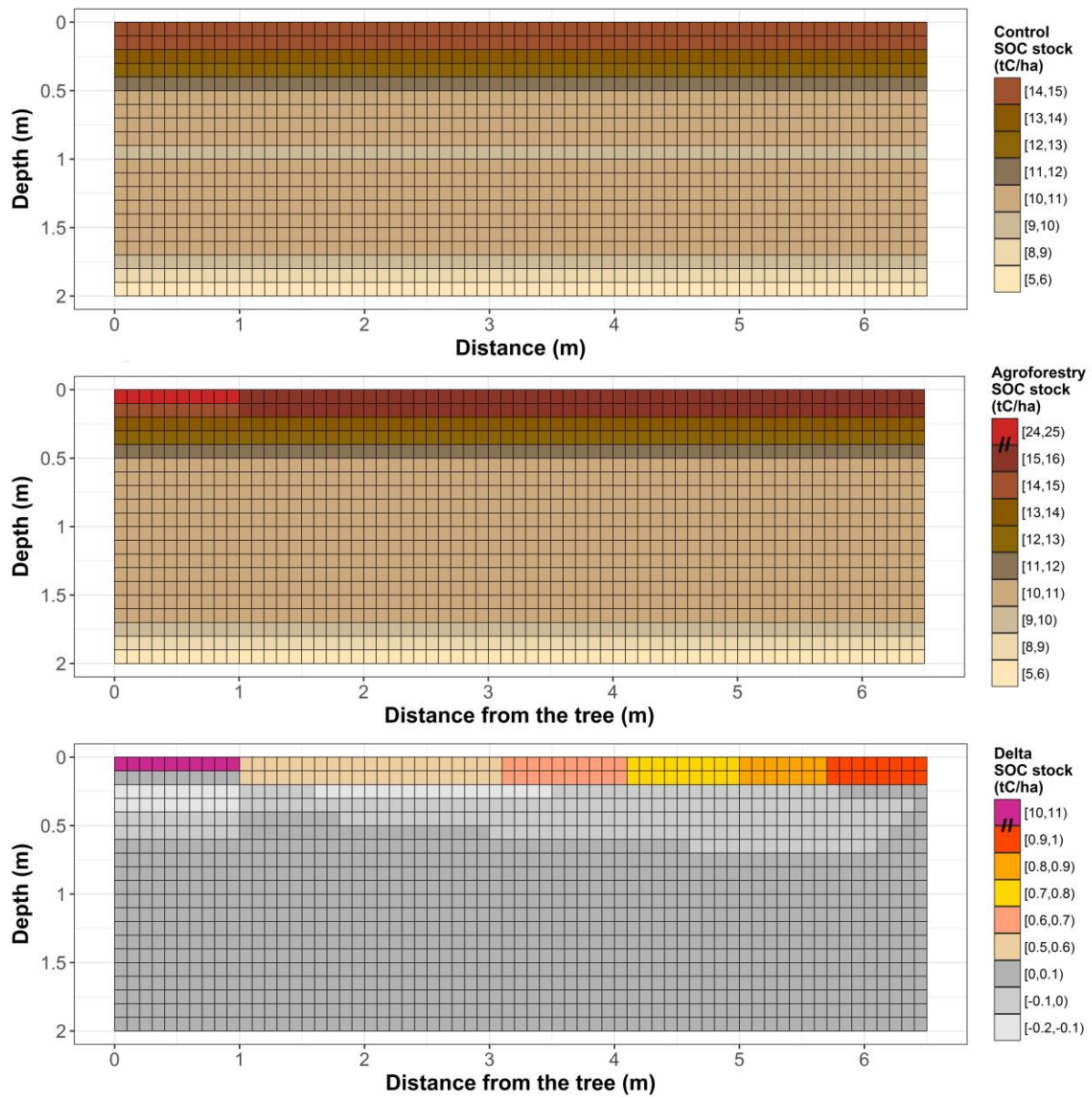
685 plot was located in the first 0.2 m depth, but SOC storage was slightly higher in the middle of  
 686 the alleys than in the alleys close to the tree rows.



687

688 **Fig. 54.** Measured and modeled soil organic carbon contents ( $\text{kg C m}^{-3}$ ) in an agricultural  
 689 control plot and in an 18-year-old silvoarable system with a two pools model without priming  
 690 effect (no *PE*), with a two pools model with priming effect (*PE*) and with a three pools model

691 without *PE*. Gray shaded bands represent standard deviations of measured SOC stocks (n=93  
 692 in the control, n=40 in the tree rows, and n=60 in the alleys).



693  
 694 **Fig. 65.** Spatial distribution of control SOC stocks (top), agroforestry SOC stocks (middle), and  
 695 additional SOC storage ( $t C ha^{-1}$ ) in an 18-year-old silvoarable system compared to an  
 696 agricultural control plot and represented by the two pools model with priming effect. The  
 697 scale used in the middle and bottom panels are not continuous due to the  
 698 large stocks predicted by the model in the top layer in the tree-row.

699

## 700 **4 Discussion**

### 701 **4.1 OC inputs drive SOC storage in agroforestry systems**

702 Increased SOC stocks in the agroforestry plot compared to the control may be explained either  
703 by increased OC inputs, or decreased OC outputs by SOC mineralization, or both. In the alleys,  
704 higher SOC stocks in the topsoil could be explained by inputs from litterfall and tree roots  
705 despite a decrease in crop inputs. Most of additional SOC storage in the agroforestry plot was  
706 found in the topsoil in the tree rows. The same distribution was observed for OC inputs to the  
707 soil. Inputs from the herbaceous vegetation had an important impact on SOC storage. The  
708 increased SOC stocks in the tree rows were largely explained by an important above-ground  
709 carbon input ( $2.13 \text{ t C ha}^{-1} \text{ yr}^{-1}$ ) by the herbaceous vegetation between trees. This result had  
710 already been suggested by Cardinael et al., (2015b) and by Cardinael et al., (2017) who showed  
711 that even young agroforestry systems could store SOC in the tree rows while trees are still very  
712 small. These “grass strips” indirectly introduced by the tree planting in parallel tree rows have  
713 a major impact on SOC stocks of agroforestry systems. Increased SOC stocks below the plough  
714 layer could be explained by higher root inputs, but these inputs could also have contributed to  
715 decrease SOC stocks below 1.5 m due to priming effect. At the plot scale, measured organic  
716 carbon inputs to the soil were increased by 40% ( $+1.1 \text{ t C ha}^{-1} \text{ yr}^{-1}$ ) down 2 m depth in the 18-  
717 year-old agroforestry plot compared to the control plot, resulting in increased SOC stocks of  
718  $3.3 \text{ t C ha}^{-1}$ . Increased OC inputs in agroforestry systems has been shown in other studies but  
719 they were only quantified in the first 20 cm of soil (Oelbermann et al., 2006; Peichl et al., 2006).  
720 This study is therefore the first one also quantifying deep OC inputs to soil. In this study and  
721 due to a lack of data, soil temperature and soil moisture were considered the same in both plots  
722 so that abiotic factors controlling SOC decomposition were identical. Reduced soil temperature  
723 is often observed in agroforestry systems (Clinch et al., 2009; Dubbert et al., 2014), but effect



724 of agroforestry on soil moisture is much more complex. The soil evaporation is reduced under  
725 the trees, but soil water is also lost through the transpiration of trees (Ilstedt et al., 2016; Ong  
726 and Leakey, 1999). These opposing effects vary with the distance from the tree (Odhiambo et  
727 al., 2001). Moreover, increased water infiltration and water storage has been observed under  
728 the trees after a rainy event (Anderson et al., 2009). Therefore, the effect of agroforestry on soil  
729 moisture is variable in time and space, and should be investigated more in details. Interactions  
730 between soil temperature and soil moisture on the SOC decomposition are known to be complex  
731 (Conant et al., 2011; Moyano et al., 2013; Sierra et al., 2015). A sensitivity analysis performed  
732 on these two boundary conditions showed that the model was not very sensitive to soil  
733 temperature and soil moisture (Fig. S3), but the real effect of these two parameters on SOC  
734 dynamics under agroforestry systems should be specifically investigated in future studies.  
735 Despite these simplifying assumptions on similarities in microclimate but also on vertical  
736 transport between the control and the agroforestry system, the model calibrated to the control  
737 plot was able to reproduce SOC stocks in tree rows and alleys and its depth distribution well.  
738 This strong validation also revealed that OC inputs were sufficient to explain the differences in  
739 SOC stocks at this site. Furthermore, the SOC decomposition rate could also be modified due  
740 to an absence of soil tillage in the tree rows (Balesdent et al., 1990) or to an increased aggregate  
741 stability (Udawatta et al., 2008) in the topsoil.

742

#### 743 **4.2 Representation of SOC spatial heterogeneity in agroforestry systems**

744 The lateral spatial heterogeneity of SOC stocks in the agroforestry plot was well described by  
745 the two pools model including priming effect, with higher SOC stocks in the tree rows' topsoil  
746 than in the alleys. The model treated the carbon from the tree row herbaceous litter as an input  
747 to the upper layer of the mineral soil, in the same way as inputs by roots. Introduction of  
748 nitrogen in the model could be further tested in order to take into account a lower carbon use

749 efficiency due to a lack of nutrients for microbial growth in this litter. The strong SOC gradient  
750 observed in the topsoil in tree rows compared to the used resolution could lead to numerical  
751 errors. We therefore tested a finer grid resolution, and results were very similar, suggesting  
752 some robustness of the model. For all models, SOC stocks were better described in the tree  
753 rows than in the alleys. In the alleys, the spatial distribution of organic inputs is more complex  
754 and thus more difficult to model. The tree root system is influenced by the soil tillage and by  
755 the competition with the crop roots, and thus the highest tree fine root density is not observed  
756 in the topsoil but in the 0.3-0.5 m soil layer (Cardinael et al., 2015a). In the model, we were not  
757 able to represent this specific tree root pattern with commonly used mathematical functions,  
758 and tree root profiles were modeled, by default, using a decreasing exponential. Indeed,  
759 piecewise linear functions introduce threshold effects not desirable for transport mechanisms,  
760 especially diffusion. This simplification could partly explain the model overestimation of SOC  
761 stocks in the 0.0-0.1 m layer of the alleys compared to observed data. This result suggests that  
762 it could be useful to couple the CARBOSAF model with a model describing root architecture  
763 and root growth (Dunbabin et al., 2013; Dupuy et al., 2010), using for instance voxel automata  
764 (Mulia et al., 2010). Moreover, the model described a slight increase of SOC stocks in the  
765 middle of the alleys than close to the trees in the alleys. This could be explained by the linear  
766 equation used to describe the crop yield as a function of the distance from the trees, leading to  
767 an overestimation of the crop yield reduction close to the trees. It could also be explained by  
768 the formalism used to model leaf litter distribution in the plot. We considered a homogeneous  
769 distribution of leaf inputs in the agroforestry plot, which was the case in the last years, but  
770 probably not in the first years of the tree growth where leaves might be more concentrated close  
771 to the trees (Thevathasan and Gordon, 1997).

772 The two pools model with priming effect also represented a slight SOC storage in the  
773 agroforestry plot below 1.0 m depth, but it was not observed in the field. This could be linked

774 to an overestimation of C input from tree fine root mortality. Indeed, a constant root turnover  
775 was considered along the soil profile, but several authors reported a decrease of the root  
776 turnover with increasing soil depth (Germon et al., 2016; Hendrick and Pregitzer, 1996; Joslin  
777 et al., 2006). However, the sensitivity analysis showed that the model was not sensitive to this  
778 parameter (Fig. S3).

779

### 780 **4.3 Vertical representation of SOC profiles in models**

781 The best model to represent SOC profiles considered the priming effect. This process can act  
782 in two different ways on the shape of SOC profiles. It has a direct effect on the SOC  
783 mineralization and it therefore modulates the amount of SOC in each soil layer, creating  
784 different SOC gradients. This indirectly affects the mechanisms of C transport within the soil  
785 profile, as shown by a modification of transport coefficients in the case of priming effect (Table  
786 5). Contrary to what was shown by Cardinael *et al.*, (2015c) in long term bare fallows receiving  
787 contrasted organic amendments, the addition of another SOC pool could not surpass the  
788 inclusion of priming effect in terms of model performance. Together with Wutzler &  
789 Reichstein, (2013) and Guenet *et al.*, (2016), this study therefore suggests that implementing  
790 priming effect into SOC models would improve model performances especially when  
791 modelling deep SOC profiles.

792 We considered here the same transport coefficients for the FOC and HSOC pools, but the  
793 quality and the size of OC particles are different, potentially leading to various movements in  
794 the soil by water fluxes or fauna activity (Lavelle, 1997). Moreover, we considered identical  
795 transport parameters in the agroforestry and in the control plot, but the presence of trees could  
796 modify soil structure, soil water fluxes (Anderson et al., 2009), and the fauna activity (Price  
797 and Gordon, 1999). However, the model was little sensitive to these parameters (Fig. S3).

798 Further study could investigate the role of different transport coefficients on the description of  
799 SOC profiles.

800

#### 801 **4.4 Higher OC inputs or a different quality of OC?**

802 The introduction of trees in an agricultural field not only modifies the amount of litter residues,  
803 but also their quality. Tree leaves, tree roots, and the herbaceous vegetation from the tree row  
804 have different C:N ratios, lignin and cellulose contents than the crop residues. Recent studies  
805 showed that plant diversity had a positive impact on SOC storage (Lange et al., 2015; Steinbeiss  
806 et al., 2008). One of the hypothesis proposed by the authors is that diverse plant communities  
807 result in more active, more abundant and more diverse microbial communities, increasing  
808 microbial products that can potentially be stabilized. In our model, litter quality is not related  
809 to different SOC pools, but is implicitly taken into account in the FOC decomposition rate,  
810 which is weighted by the respective contribution from the different types of OC inputs. To test  
811 this, we performed a model run considering that all OC inputs in the agroforestry plot were crop  
812 inputs (all FOC decomposition rates equaled wheat decomposition rate), but results were not  
813 significantly different from the one presented here. Hence, we considered that changes in litter  
814 quality in the agroforestry plot did not significantly influence SOC decomposition rates.

815

#### 816 **4.5 Possible limitation of SOC storage by priming effect**

817 Our modelling results suggested that the priming effect could considerably reduce the capacity  
818 of soils to store organic carbon. Our study showed that the increase of SOC stocks was not  
819 proportional to OC inputs, especially at depth. This result has often been observed in Free Air  
820 CO<sub>2</sub> Enrichment (FACE) experiments. In these experiments, productivity is usually increased  
821 due to CO<sub>2</sub> fertilization, but several authors also reported an increase in SOC decomposition  
822 but not linearly linked to the productivity increase (van Groenigen et al., 2014; Sulman et al.,

823 2014). In a long-term FACE experiment, Carney *et al.*, (2007) also found that SOC decreased  
824 due to priming effect, offsetting 52% of additional carbon accumulated in aboveground and  
825 coarse root biomass. The priming effect intensity also relies on nutrient availability (Zhang *et*  
826 *al.*, 2013). In agroforestry systems, tree roots can intercept leached nitrate below the crop  
827 rooting zone (Andrianarisoa *et al.*, 2016), reducing nutrient availability. This beneficial  
828 ecosystem service could indirectly increase the priming effect intensity in deep soil layers.  
829 The formalism used here to simulate priming effect assumes that there is no mineralisation of  
830 the SOC in the absence of fresh OC inputs (no basal respiration). This is a strong hypothesis,  
831 but this situation never occurs since the FOC pool is never empty (data not shown). In the alleys  
832 and below the maximum rooting depth of crops, there are no direct inputs of FOC, but OC is  
833 transported in these deep layers due to transport mechanisms. However, further studies could  
834 study the impact of the priming effect formalism on the estimation of its intensity by using  
835 explicit microbial biomass for instance (Blagodatsky *et al.*, 2010; Perveen *et al.*, 2014).  
836 Finally, root exudates were not quantified in this study. Several authors showed that they could  
837 induce strong priming effects (Bengtson *et al.*, 2012; Keiluweit *et al.*, 2015), but root exudates  
838 are also a source of labile carbon, potentially contributing to stable SOC (Cotrufo *et al.*, 2013).  
839 These opposing effects of root exudates on SOC should be further investigated, especially  
840 concerning the deep roots in agroforestry systems.

841

## 842 **5 Conclusions**

843 We proposed the first model that simulates soil organic carbon dynamics in agroforestry  
844 accounting for both the whole soil profile and the lateral spatial heterogeneity in agroforestry  
845 plots. The two pools model with priming effect described reasonably well the measured SOC  
846 stocks after 18 years of agroforestry and SOC distributions with depth. It showed that the  
847 increased inputs of fresh biomass to soil in the agroforestry system explained the observed

848 additional SOC storage and suggested priming effect as a process controlling SOC stocks in the  
849 presence of trees. This study points out at processes that may be modified by deep rooting trees  
850 and deserve further studies given their potential effects on SOC dynamics, such as additional  
851 inputs of C as roots exudates, or altered soil structure leading to modified SOC transport rates.

852

## 853 **6 Data availability**

854 The data and the model are freely available upon request and can be obtained by contacting the  
855 author (remi.cardinael@cirad.fr).

856

## 857 **Information about the Supplement**

858 The Supplement includes the walnut tree fine root biomass (Table S1), [the covariance matrices](#)  
859 [P<sub>b</sub> of optimized parameters \(Table S2\)](#), the different model performances (Table S32), the  
860 potential SOC decomposition rate as a function of soil depth (Fig. S1), the correlation ~~matrix~~  
861 [matrices](#) of optimized parameters (Fig. S2), and a sensitivity analysis of the model (Fig. S3).

862

## 863 *Acknowledgments.*

864 This study was financed by the French Environment and Energy Management Agency  
865 (ADEME), following a call for proposals as part of the REACCTIF program (Research on  
866 Climate Change Mitigation in Agriculture and Forestry). This work was part of the funded  
867 project AGRIPSOL (Agroforestry for Soil Protection, 1260C0042), coordinated by Agroof.  
868 Rémi Cardinael was supported both by ADEME and by La Fondation de France. We thank the  
869 farmer, Mr Breton, who allowed us to sample in his field. We are very grateful to our colleagues  
870 for their work in the field since the tree planting, especially Jean-François Bourdoncle, Myriam  
871 Dauzat, Lydie Dufour, Jonathan Mineau, Alain Sellier and Benoit Suard. We thank colleagues  
872 and students who helped us for measurements in the field or in the laboratory, especially Daniel

873 Billiou, Cyril Girardin, Patricia Mahafaka, Agnès Martin, Valérie Pouteau, Alexandre Rosa,  
874 and Manon Villeneuve. Finally, we would like to thank Jérôme Balesdent, Pierre Barré and  
875 Philippe Peylin for their valuable comments on the modeling part of this work.

876

## 877 **References**

878 Ahrens, B., Braakhekke, M. C., Guggenberger, G., Schrumpf, M. and Reichstein, M.:  
879 Contribution of sorption, DOC transport and microbial interactions to the  $^{14}\text{C}$  age of a soil  
880 organic carbon profile: Insights from a calibrated process model, *Soil Biol. Biochem.*, 88, 390–  
881 402.

882 Albrecht, A. and Kandji, S. T.: Carbon sequestration in tropical agroforestry systems, *Agric.*  
883 *Ecosyst. Environ.*, 99, 15–27, 2003.

884 Anderson, S. H., Udawatta, R. P., Seobi, T. and Garrett, H. E.: Soil water content and infiltration  
885 in agroforestry buffer strips, *Agrofor. Syst.*, 75(1), 5–16, 2009.

886 Andrianarisoa, K., Dufour, L., Bienaime, S., Zeller, B. and Dupraz, C.: The introduction of  
887 hybrid walnut trees (*Juglans nigra* x *regia* cv. NG23) into cropland reduces soil mineral N  
888 content in autumn in southern France, *Agrofor. Syst.*, 90(2), 193–205, 2016.

889 Baisden, W. T. and Parfitt, R. L.: Bomb  $^{14}\text{C}$  enrichment indicates decadal C pool in deep soil?,  
890 *Biogeochemistry*, 85, 59–68, 2007.

891 Baisden, W. T., Amundson, R., Brenner, D. L., Cook, A. C., Kendall, C. and Harden, J. W.: A  
892 multiisotope C and N modeling analysis of soil organic matter turnover and transport as a  
893 function of soil depth in a California annual grassland soil chronosequence, *Global*  
894 *Biogeochem. Cycles*, 16(4), 82-1-82–26, 2002.

895 Balandier, P. and Dupraz, C.: Growth of widely spaced trees. A case study from young  
896 agroforestry plantations in France, *Agrofor. Syst.*, 43, 151–167, 1999.

897 Balesdent, J., Mariotti, A. and Boissgonnier, D.: Effect of tillage on soil organic carbon  
898 mineralization estimated from  $^{13}\text{C}$  abundance in maize fields, *J. Soil Sci.*, 41(4), 587–596, 1990.

899 Bambrick, A. D., Whalen, J. K., Bradley, R. L., Cogliastro, A., Gordon, A. M., Olivier, A. and  
900 Thevathasan, N. V: Spatial heterogeneity of soil organic carbon in tree-based intercropping  
901 systems in Quebec and Ontario, Canada, *Agrofor. Syst.*, 79, 343–353, 2010.

902 Bengtson, P., Barker, J. and Grayston, S. J.: Evidence of a strong coupling between root  
903 exudation, C and N availability, and stimulated SOM decomposition caused by rhizosphere  
904 priming effects, *Ecol. Evol.*, 2(8), 1843–1852, 2012.

905 Blagodatsky, S., Blagodatskaya, E., Yuyukina, T. and Kuzyakov, Y.: Model of apparent and  
906 real priming effects: Linking microbial activity with soil organic matter decomposition, *Soil*  
907 *Biol. Biochem.*, 42(8), 1275–1283, 2010.

908 Braakhekke, M. C., Beer, C., Hoosbeek, M. R., Reichstein, M., Kruijt, B., Schrumppf, M. and  
909 Kabat, P.: SOMPROF: A vertically explicit soil organic matter model, *Ecol. Modell.*, 222(10),  
910 1712–1730, 2011.

911 Bruun, S., Christensen, B. T., Thomsen, I. K., Jensen, E. S. and Jensen, L. S.: Modeling vertical  
912 movement of organic matter in a soil incubated for 41 years with  $^{14}\text{C}$  labeled straw, *Soil Biol.*  
913 *Biochem.*, 39(1), 368–371, 2007.

914 Burgess, P. J., Incoll, L. D., Corry, D. T., Beaton, A. and Hart, B. J.: Poplar (*Populus* spp)  
915 growth and crop yields in a silvoarable experiment at three lowland sites in England, *Agrofor.*  
916 *Syst.*, 63, 157–169, 2004.

917 Cardinael, R., Mao, Z., Prieto, I., Stokes, A., Dupraz, C., Kim, J. H. and Jourdan, C.:  
918 Competition with winter crops induces deeper rooting of walnut trees in a Mediterranean alley  
919 cropping agroforestry system, *Plant Soil*, 391, 219–235, 2015a.

920 Cardinael, R., Chevallier, T., Barthès, B. G., Saby, N. P. A., Parent, T., Dupraz, C., Bernoux,



921 M. and Chenu, C.: Impact of alley cropping agroforestry on stocks, forms and spatial  
922 distribution of soil organic carbon - A case study in a Mediterranean context, *Geoderma*, 259–  
923 260, 288–299, 2015b.

924 Cardinael, R., Eglin, T., Guenet, B., Neill, C., Houot, S. and Chenu, C.: Is priming effect a  
925 significant process for long-term SOC dynamics? Analysis of a 52-years old experiment,  
926 *Biogeochemistry*, 123, 203–219, 2015c.

927 Cardinael, R., Chevallier, T., Cambou, A., Béral, C., Barthès, B. G., Dupraz, C., Durand, C.,  
928 Kouakoua, E. and Chenu, C.: Increased soil organic carbon stocks under agroforestry: A survey  
929 of six different sites in France, *Agric. Ecosyst. Environ.*, 236, 243–255, 2017.

930 Carney, K. M., Hungate, B. A., Drake, B. G. and Megonigal, J. P.: Altered soil microbial  
931 community at elevated CO<sub>2</sub> leads to loss of soil carbon, *PNAS*, 104(12), 4990–4995, 2007.

932 Charbonnier, F., le Maire, G., Dreyer, E., Casanoves, F., Christina, M., Dauzat, J., Eitel, J. U.  
933 H., Vaast, P., Vierling, L. A. and Roupsard, O.: Competition for light in heterogeneous  
934 canopies: Application of MAESTRA to a coffee (*Coffea arabica* L.) agroforestry system,  
935 *Agric. For. Meteorol.*, 181, 152–169, 2013.

936 Chaudhry, A. K., Khan, G. S., Siddiqui, M. T., Akhtar, M. and Aslam, Z.: Effect of arable crops  
937 on the growth of poplar (*Populus deltoides*) tree in agroforestry system, *Pakistan J. Agric. Sci.*,  
938 40, 82–85, 2003.

939 Chiffot, V., Bertoni, G., Cabanettes, A. and Gavaland, A.: Beneficial effects of intercropping  
940 on the growth and nitrogen status of young wild cherry and hybrid walnut trees, *Agrofor. Syst.*,  
941 66(1), 13–21, 2006.

942 Clinch, R. L., Thevathasan, N. V., Gordon, A. M., Volk, T. A. and Sidders, D.: Biophysical  
943 interactions in a short rotation willow intercropping system in southern Ontario, Canada, *Agric.*  
944 *Ecosyst. Environ.*, 131(1–2), 61–69, 2009.

945 Conant, R. T., Ryan, M. G., Ågren, G. I., Birge, H. E., Davidson, E. A., Eliasson, P. E., Evans,  
946 S. E., Frey, S. D., Giardina, C. P., Hopkins, F. M., Hyvönen, R., Kirschbaum, M. U. F.,  
947 Lavallee, J. M., Leifeld, J., Parton, W. J., Megan Steinweg, J., Wallenstein, M. D., Martin  
948 Wetterstedt, J. Å. and Bradford, M. A.: Temperature and soil organic matter decomposition  
949 rates - synthesis of current knowledge and a way forward, *Glob. Chang. Biol.*, 17(11), 3392–  
950 3404, 2011.

951 Cotrufo, M. F., Wallenstein, M. D., Boot, C. M., Deneff, K. and Paul, E.: The Microbial  
952 Efficiency-Matrix Stabilization (MEMS) framework integrates plant litter decomposition with  
953 soil organic matter stabilization: do labile plant inputs form stable soil organic matter?, *Glob.*  
954 *Chang. Biol.*, 19(4), 988–95, 2013.

955 Davidson, E. A. and Janssens, I. A.: Temperature sensitivity of soil carbon decomposition and  
956 feedbacks to climate change, *Nature*, 440, 165–173, 2006.

957 Dimassi, B., Cohan, J.-P., Labreuche, J. and Mary, B.: Changes in soil carbon and nitrogen  
958 following tillage conversion in a long-term experiment in Northern France, *Agric. Ecosyst.*  
959 *Environ.*, 169, 12–20, 2013.

960 Dubbert, M., Mosena, A., Piayda, A., Cuntz, M., Correia, A. C., Pereira, J. S. and Werner, C.:  
961 Influence of tree cover on herbaceous layer development and carbon and water fluxes in a  
962 Portuguese cork-oak woodland, *Acta Oecologica*, 59, 35–45, 2014.

963 Dufour, L., Metay, A., Talbot, G. and Dupraz, C.: Assessing Light Competition for Cereal  
964 Production in Temperate Agroforestry Systems using Experimentation and Crop Modelling, *J.*  
965 *Agron. Crop Sci.*, 199(3), 217–227, 2013.

966 Dunbabin, V. M., Postma, J. A., Schnepf, A., Pagès, L., Javaux, M., Wu, L., Leitner, D., Chen,  
967 Y. L., Rengel, Z. and Diggle, A. J.: Modelling root-soil interactions using three-dimensional  
968 models of root growth, architecture and function, *Plant Soil*, 372(1–2), 93–124, 2013.

969 Dupuy, L., Gregory, P. J. and Bengough, A. G.: Root growth models: Towards a new generation  
970 of continuous approaches, *J. Exp. Bot.*, 61(8), 2131–2143, 2010.

971 Duursma, R. and Medlyn, B.: MAESPA: a model to study interactions between water  
972 limitation, environmental drivers and vegetation function at tree and stand levels, with an  
973 example application to  $[\text{CO}_2] \times$  drought interactions, *Geosci. Model Dev.*, 5, 919–940, 2012.

974 Eilers, K. G., Debenport, S., Anderson, S. and Fierer, N.: Digging deeper to find unique  
975 microbial communities: The strong effect of depth on the structure of bacterial and archaeal  
976 communities in soil, *Soil Biol. Biochem.*, 50, 58–65, 2012.

977 Eissenstat, D. M. and Yanai, R. D.: The Ecology of Root Lifespan, *Adv. Ecol. Res.*, 27, 1–60,  
978 1997.

979 Ellert, B. H. and Bettany, J. R.: Calculation of organic matter and nutrients stored in soils under  
980 contrasting management regimes, *Can. J. Soil Sci.*, 75, 529–538, 1995.

981 Elzein, A. and Balesdent, J.: Mechanistic simulation of vertical distribution of carbon  
982 concentrations and residence times in soils, *Soil Sci. Soc. Am. J.*, 59, 1328–1335, 1995.

983 Fierer, N., Schimel, J. P. and Holden, P. A.: Variations in microbial community composition  
984 through two soil depth profiles, *Soil Biol. Biochem.*, 35(1), 167–176, 2003.

985 Fontaine, S., Barot, S., Barré, P., Bdioui, N., Mary, B. and Rumpel, C.: Stability of organic  
986 carbon in deep soil layers controlled by fresh carbon supply, *Nature*, 450, 277–281, 2007.

987 Germon, A., Cardinael, R., Prieto, I., Mao, Z., Kim, J. H., Stokes, A., Dupraz, C., Laclau, J.-P.  
988 and Jourdan, C.: Unexpected phenology and lifespan of shallow and deep fine roots of walnut  
989 trees grown in a silvoarable Mediterranean agroforestry system, *Plant Soil*, 401, 409–426, 2016.

990 Graves, A. R., Burgess, P. J., Palma, J. H. N., Herzog, F., Moreno, G., Bertomeu, M., Dupraz,  
991 C., Liagre, F., Keesman, K., van der Werf, W., de Nooy, a. K. and van den Briel, J. P.:  
992 Development and application of bio-economic modelling to compare silvoarable, arable, and

993 forestry systems in three European countries, *Ecol. Eng.*, 29(4), 434–449, 2007.

994 Graves, A. R., Burgess, P. J., Palma, J., Keesman, K. J., van der Werf, W., Dupraz, C., van  
995 Keulen, H., Herzog, F. and Mayus, M.: Implementation and calibration of the parameter-sparse  
996 Yield-SAFE model to predict production and land equivalent ratio in mixed tree and crop  
997 systems under two contrasting production situations in Europe, *Ecol. Modell.*, 221, 1744–1756,  
998 2010.

999 van Groenigen, K. J., Qi, X., Osenberg, C. W., Luo, Y. and Hungate, B. A.: Faster  
1000 decomposition under increased atmospheric CO<sub>2</sub> limits soil carbon storage, *Science.*, 344, 508–  
1001 509, 2014.

1002 Guenet, B., Eglin, T., Vasilyeva, N., Peylin, P., Ciais, P. and Chenu, C.: The relative importance  
1003 of decomposition and transport mechanisms in accounting for soil organic carbon profiles,  
1004 *Biogeosciences*, 10(4), 2379–2392, 2013.

1005 Guenet, B., Moyano, F. E., Peylin, P., Ciais, P. and Janssens, I. A.: Towards a representation  
1006 of priming on soil carbon decomposition in the global land biosphere model ORCHIDEE  
1007 (version 1.9.5.2), *Geosci. Model Dev.*, 9, 841–855, 2016.

1008 Haile, S. G., Nair, V. D. and Nair, P. K. R.: Contribution of trees to carbon storage in soils of  
1009 silvopastoral systems in Florida, USA, *Glob. Chang. Biol.*, 16, 427–438, 2010.

1010 Hendrick, R. L. and Pregitzer, K. S.: Temporal and depth-related patterns of fine root dynamics  
1011 in northern hardwood forests, *J. Ecol.*, 84, 167–176, 1996.

1012 Howlett, D. S., Moreno, G., Mosquera Losada, M. R., Nair, P. K. R. and Nair, V. D.: Soil  
1013 carbon storage as influenced by tree cover in the Dehesa cork oak silvopasture of central-  
1014 western Spain, *J. Environ. Monit.*, 13(7), 1897–904, 2011.

1015 Ilstedt, U., Bargués Tobella, A., Bazié, H. R., Bayala, J., Verbeeten, E., Nyberg, G., Sanou, J.,  
1016 Benegas, L., Murdiyarso, D., Laudon, H., Sheil, D. and Malmer, A.: Intermediate tree cover

1017 can maximize groundwater recharge in the seasonally dry tropics, *Sci. Rep.*, 6, 21930, 2016.

1018 IUSS Working Group WRB: World Reference Base for Soil Resources 2006, first update 2007.

1019 World Soil Resources Reports No. 103. FAO, Rome., 2007.

1020 Jobbagy, E. G. and Jackson, R. B.: The vertical distribution of soil organic carbon and its  
1021 relation to climate and vegetation, *Ecol. Appl.*, 10, 423–436, 2000.

1022 Joslin, J. D., Gaudinski, J. B., Torn, M. S., Riley, W. J. and Hanson, P. J.: Fine-root turnover  
1023 patterns and their relationship to root diameter and soil depth in a <sup>14</sup>C-labeled hardwood forest,  
1024 *New Phytol.*, 172, 523–535, 2006.

1025 Kätterer, T., Bolinder, M. A., Andrén, O., Kirchmann, H. and Menichetti, L.: Roots contribute  
1026 more to refractory soil organic matter than above-ground crop residues, as revealed by a long-  
1027 term field experiment, *Agric. Ecosyst. Environ.*, 141, 184–192, 2011.

1028 Keiluweit, M., Bougoure, J. J., Nico, P. S., Pett-Ridge, J., Weber, P. K. and Kleber, M.: Mineral  
1029 protection of soil carbon counteracted by root exudates, *Nat. Clim. Chang.*, 5, 588–595, 2015.

1030 Kim, D.-G., Kirschbaum, M. U. F. and Beedy, T. L.: Carbon sequestration and net emissions  
1031 of CH<sub>4</sub> and N<sub>2</sub>O under agroforestry: Synthesizing available data and suggestions for future  
1032 studies, *Agric. Ecosyst. Environ.*, 226, 65–78, 2016.

1033 Koarashi, J., Hockaday, W. C., Masiello, C. A. and Trumbore, S. E.: Dynamics of decadal  
1034 cycling carbon in subsurface soils, *J. Geophys. Res.*, 117, 1–13, 2012.

1035 Koven, C. D., Riley, W. J., Subin, Z. M., Tang, J. Y., Torn, M. S., Collins, W. D., Bonan, G.  
1036 B., Lawrence, D. M. and Swenson, S. C.: The effect of vertically resolved soil biogeochemistry  
1037 and alternate soil C and N models on C dynamics of CLM4, *Biogeosciences*, 10(11), 7109–  
1038 7131, 2013.

1039 Lange, M., Eisenhauer, N., Sierra, C. A., Bessler, H., Engels, C., Griffiths, R. I., Mellado-  
1040 Vázquez, P. G., Malik, A. A., Roy, J., Scheu, S., Steinbeiss, S., Thomson, B. C., Trumbore, S.

1041 E. and Gleixner, G.: Plant diversity increases soil microbial activity and soil carbon storage,  
1042 *Nat. Commun.*, 6, 6707, 2015.

1043 Lavelle, P.: Faunal activities and soil processes: adaptative strategy that determine ecosystem  
1044 function., 1997.

1045 Li, F., Meng, P., Fu, D. and Wang, B.: Light distribution, photosynthetic rate and yield in a  
1046 *Paulownia-wheat intercropping system in China*, *Agrofor. Syst.*, 74(2), 163–172, 2008.

1047 Lorenz, K. and Lal, R.: Soil organic carbon sequestration in agroforestry systems. A review,  
1048 *Agron. Sustain. Dev.*, 34, 443–454, 2014.

1049 Luedeling, E., Smethurst, P. J., Baudron, F., Bayala, J., Huth, N. I., van Noordwijk, M., Ong,  
1050 C. K., Mulia, R., Lusiana, B., Muthuri, C. and Sinclair, F. L.: Field-scale modeling of tree-crop  
1051 interactions: Challenges and development needs, *Agric. Syst.*, 142, 51–69, 2016.

1052 Mead, R. and Willey, R. W.: The concept of a “land equivalent ratio” and advantages in yields  
1053 from intercropping, *Exp. Agric.*, 16(3), 217–228, 1980.

1054 Moreno, G., Obrador, J. J., Cubera, E. and Dupraz, C.: Fine root distribution in Dehesas of  
1055 central-western Spain, *Plant Soil*, 277(1–2), 153–162, 2005.

1056 Moyano, F. E., Vasilyeva, N., Bouckaert, L., Cook, F., Craine, J., Curiel Yuste, J., Don, A.,  
1057 Epron, D., Formanek, P., Franzluebbers, A., Ilstedt, U., Kätterer, T., Orchard, V., Reichstein,  
1058 M., Rey, A., Ruamps, L., Subke, J. A., Thomsen, I. K. and Chenu, C.: The moisture response  
1059 of soil heterotrophic respiration: Interaction with soil properties, *Biogeosciences*, 9, 1173–  
1060 1182, 2012.

1061 Moyano, F. E., Manzoni, S. and Chenu, C.: Responses of soil heterotrophic respiration to  
1062 moisture availability: An exploration of processes and models, *Soil Biol. Biochem.*, 59, 72–85,  
1063 2013.

1064 Mulia, R. and Dupraz, C.: Unusual fine root distributions of two deciduous tree species in

1065 southern France: What consequences for modelling of tree root dynamics?, *Plant Soil*, 281, 71–  
1066 85, 2006.

1067 Mulia, R., Dupraz, C. and van Noordwijk, M.: Reconciling root plasticity and architectural  
1068 ground rules in tree root growth models with voxel automata, *Plant Soil*, 337(1–2), 77–92, 2010.

1069 Nair, P. K.: *An introduction to agroforestry*, Kluwer Academic Publishers, Dordrecht, The  
1070 Netherlands., 1993.

1071 Nair, P. K. R.: Classification of agroforestry systems, *Agrofor. Syst.*, 3(2), 97–128, 1985.

1072 van Noordwijk, M. and Lusiana, B.: WaNuLCAS, a model of water, nutrient and light capture  
1073 in agroforestry systems, *Agrofor. Syst.*, 43, 217–242, 1999.

1074 Odhiambo, H. O., Ong, C. K., Deans, J. D., Wilson, J., Khan, A. A. H. and Sprent, J. I.: Roots,  
1075 soil water and crop yield: Tree crop interactions in a semi-arid agroforestry system in Kenya,  
1076 *Plant Soil*, 235(2), 221–233, 2001.

1077 Oelbermann, M. and Voroney, R. P.: An evaluation of the century model to predict soil  
1078 organic carbon: examples from Costa Rica and Canada, *Agrofor. Syst.*, 82, 37–50, 2011.

1079 Oelbermann, M., Voroney, R. P. and Gordon, A. M.: Carbon sequestration in tropical and  
1080 temperate agroforestry systems: a review with examples from Costa Rica and southern Canada,  
1081 *Agric. Ecosyst. Environ.*, 104, 359–377, 2004.

1082 Oelbermann, M., Voroney, R. P., Thevathasan, N. V., Gordon, A. M., Kass, D. C. L. and  
1083 Schlönvoigt, A. M.: Soil carbon dynamics and residue stabilization in a Costa Rican and  
1084 southern Canadian alley cropping system, *Agrofor. Syst.*, 68(1), 27–36, 2006.

1085 Ong, C. K. and Leakey, R. R. B.: Why tree-crop interactions in agroforestry appear at odds with  
1086 tree-grass interactions in tropical savannahs, *Agrofor. Syst.*, 45(1–3), 109–129, 1999.

1087 Parton, W. J., Schimel, D. S., Cole, C. V and Ojima, D. S.: Analysis of factors controlling soil  
1088 organic matter levels in great plains grasslands, *Soil Sci. Soc. Am. J.*, 51, 1173–1179, 1987.

1089 Peichl, M., Thevathasan, N. V, Gordon, A. M., Huss, J. and Abohassan, R. A.: Carbon  
1090 sequestration potentials in temperate tree-based intercropping systems, southern Ontario,  
1091 Canada, *Agrofor. Syst.*, 66, 243–257, 2006.

1092 Perveen, N., Barot, S., Alvarez, G., Klumpp, K., Martin, R., Rapaport, A., Herfurth, D.,  
1093 Louault, F. and Fontaine, S.: Priming effect and microbial diversity in ecosystem functioning  
1094 and response to global change: A modeling approach using the SYMPHONY model, *Glob.*  
1095 *Chang. Biol.*, 20(4), 1174–1190, 2014.

1096 Price, G. W. and Gordon, A. M.: Spatial and temporal distribution of earthworms in a temperate  
1097 intercropping system in southern Ontario, Canada, *Agrofor. Syst.*, 44, 141–149, 1999.

1098 Prieto, I., Roumet, C., Cardinael, R., Kim, J., Maeght, J.-L., Mao, Z., Portillo, N.,  
1099 Thammahacksa, C., Dupraz, C., Jourdan, C., Pierret, A., Roupsard, O. and Stokes, A.: Root  
1100 functional parameters along a land-use gradient: evidence of a community-level economics  
1101 spectrum, *J. Ecol.*, 103, 361–373, 2015.

1102 Prieto, I., Stokes, A. and Roumet, C.: Root functional parameters predict fine root  
1103 decomposability at the community level, *J. Ecol.*, 104, 725–733, 2016.

1104 R Development Core Team: R: A language and environment for statistical computing, 2013.

1105 Rasse, D. P., Mulder, J., Moni, C. and Chenu, C.: Carbon turnover kinetics with depth in a  
1106 French loamy soil, *Soil Sci. Soc. Am. J.*, 70, 2097–2105, 2006.

1107 Salomé, C., Nunan, N., Pouteau, V., Lerch, T. Z. and Chenu, C.: Carbon dynamics in topsoil  
1108 and in subsoil may be controlled by different regulatory mechanisms, *Glob. Chang. Biol.*, 16,  
1109 416–426, 2010.

1110 Santaren, D., Peylin, P., Viovy, N. and Ciais, P.: Optimizing a process-based ecosystem model  
1111 with eddy-covariance flux measurements: A pine forest in southern France, *Global*  
1112 *Biogeochem. Cycles*, 21, 1–15, 2007.



1113 Schwarz, G.: Estimating dimension of a model, *Ann. Stat.*, 6(2), 461–464, 1978.

1114 Shahzad, T., Chenu, C., Genet, P., Barot, S., Perveen, N., Mougin, C. and Fontaine, S.:  
1115 Contribution of exudates, arbuscular mycorrhizal fungi and litter depositions to the rhizosphere  
1116 priming effect induced by grassland species, *Soil Biol. Biochem.*, 80, 146–155, 2015.

1117 Sierra, C. A., Trumbore, S. E., Davidson, E. A., Vicca, S. and Janssens, I.: Sensitivity of  
1118 decomposition rates of soil organic matter with respect to simultaneous changes in temperature  
1119 and moisture, *J. Adv. Model. Earth Syst.*, 7, 335–356, 2015.

1120 Soetaert, K., Petzoldt, T. and Woodrow Setzer, R.: Solving Differential Equations in R:  
1121 Package deSolve, *J. Stat. Softw.*, 33(9), 1–25, 2010.

1122 Somarriba, E.: Revisiting the past: an essay on agroforestry definition, *Agrofor. Syst.*, 19(3),  
1123 233–240, 1992.

1124 Steinbeiss, S., Beßler, H., Engels, C., Temperton, V. M., Buchmann, N., Roscher, C.,  
1125 Kreuziger, Y., Baade, J., Habekost, M. and Gleixner, G.: Plant diversity positively affects  
1126 short-term soil carbon storage in experimental grasslands, *Glob. Chang. Biol.*, 14(12), 2937–  
1127 2949, 2008.

1128 Sulman, B. N., Phillips, R. P., Oishi, A. C., Shevliakova, E. and Pacala, S. W.: Microbe-driven  
1129 turnover offsets mineral-mediated storage of soil carbon under elevated CO<sub>2</sub>, *Nat. Clim.*  
1130 *Chang.*, 4, 1099–1102, 2014.

1131 Taghizadeh-Toosi, A., Christensen, B. T., Hutchings, N. J., Vejlin, J., Kätterer, T., Glendining,  
1132 M. and Olesen, J. E.: C-TOOL: A simple model for simulating whole-profile carbon storage in  
1133 temperate agricultural soils, *Ecol. Modell.*, 292, 11–25, 2014.

1134 Talbot, G.: L'intégration spatiale et temporelle du partage des ressources dans un système  
1135 agroforestier noyers-céréales: une clef pour en comprendre la productivité ?, PhD Dissertation,  
1136 Université Montpellier II., 2011.

1137 Tarantola, A.: Inverse problem theory: methods for data fitting and model parameter estimation,  
1138 edited by Elsevier., 1987.

1139 Tarantola, A.: Inverse Problem Theory and Methods for Model Parameter Estimation, edited  
1140 by SIAM., 2005.

1141 Thevathasan, N. V. and Gordon, A. M.: Poplar leaf biomass distribution and nitrogen dynamics  
1142 in a poplar-barley intercropped system in southern Ontario, Canada, *Agrofor. Syst.*, 37, 79–90,  
1143 1997.

1144 Udawatta, R. P., Kremer, R. J., Adamson, B. W. and Anderson, S. H.: Variations in soil  
1145 aggregate stability and enzyme activities in a temperate agroforestry practice, *Appl. Soil Ecol.*,  
1146 39(2), 153–160, 2008.

1147 Virto, I., Barré, P., Burlot, A. and Chenu, C.: Carbon input differences as the main factor  
1148 explaining the variability in soil organic C storage in no-tilled compared to inversion tilled  
1149 agrosystems, *Biogeochemistry*, 108, 17–26, 2012.

1150 van der Werf, W., Keesman, K., Burgess, P., Graves, A., Pilbeam, D., Incoll, L. D., Metselaar,  
1151 K., Mayus, M., Stappers, R., van Keulen, H., Palma, J. and Dupraz, C.: Yield-SAFE: A  
1152 parameter-sparse, process-based dynamic model for predicting resource capture, growth, and  
1153 production in agroforestry systems, *Ecol. Eng.*, 29(4), 419–433, 2007.

1154 Wutzler, T. and Reichstein, M.: Colimitation of decomposition by substrate and decomposers  
1155 - a comparison of model formulations, *Biogeosciences*, 5, 749–759, 2008.

1156 Wutzler, T. and Reichstein, M.: Priming and substrate quality interactions in soil organic matter  
1157 models, *Biogeosciences*, 10(3), 2089–2103, 2013.

1158 Yin, R. and He, Q.: The spatial and temporal effects of paulownia intercropping: The case of  
1159 northern China, *Agrofor. Syst.*, 37, 91–109, 1997.

1160 Zhang, W., Wang, X. and Wang, S.: Addition of external organic carbon and native soil organic

1161 carbon decomposition: a meta-analysis., PLoS One, 8(2), e54779, 2013.

1162

1163

1164

1165

1166

1167

1168

1169

1170

1171

1172

1173

1174

1175

1176

1177